AMERICAN MUSEUM NOVITATES

Number 3958, 43 pp. September 5, 2020

Systematics of Neotropical Spiny Mice, Genus *Neacomys* Thomas, 1900 (Rodentia: Cricetidae), from Southeastern Amazonia, with Descriptions of Three New Species

THIAGO BORGES FERNANDES SEMEDO,[1, 2] MARIA NAZARETH FERREIRA DA SILVA,[3] ELIÉCER E. GUTIÉRREZ,[4] DANIELA CRISTINA FERREIRA,[1] MARIO DA SILVA NUNES,[5] ANA CRISTINA MENDES-OLIVEIRA,[6] IZENI PIRES FARIAS,[5] AND ROGÉRIO VIEIRA ROSSI[1]

ABSTRACT

Species of *Neacomys* are small cricetid rodents that occur in forested habitats of Central and South America, from eastern Panama to central Bolivia and central/western Brazil. In order to assess species diversity of this poorly known genus, we obtained cytochrome *b* gene sequences from the most comprehensive taxonomic and geographic sampling analyzed to date. We also conducted morphological analyses on a large series of specimens housed in 15 museums, including types of 10 out of 14 nominal taxa. Our analyses of the genetic data recovered 17

[1] Programa de Pós-graduação em Zoologia, Instituto de Biociências, Universidade Federal de Mato Grosso (UFMT), Cuiabá, Brazil.
[2] Instituto Nacional de Pesquisa do Pantanal (INPP), Museu Paraense Emílio Goeldi (MPEG) - Programa de Capacitação Institucional, Cuiabá, Brazil.
[3] Coleção de Mamíferos, Instituto Nacional de Pesquisas da Amazônia (INPA), Manaus, Brazil.
[4] Programa de Pós-Graduação em Biodiversidade Animal, Centro de Ciências Naturais e Exatas, Universidade Federal de Santa Maria (UFSM), Santa Maria, Brazil.
[5] Laboratório de Evolução e Genética Animal (LEGAL), Departamento de Genética, Universidade Federal do Amazonas (UFAM), Manaus, Brazil.
[6] Instituto de Ciências Biológicas - LABEV, Universidade Federal do Pará (UFPA), Belém, Brazil.

 ISSN 0003-0082

lineages clustered in four distinct clades. Among these lineages, 11 correspond to species currently recognized as valid, and the remaining six are putative new species. In southeastern Amazonia—the geographical scope of this report—four undescribed species were discovered, three of which are named herein: *Neacomys marajoara*, sp. nov., from the Island of Marajó, Pará state; *Neacomys vossi*, sp. nov., restricted to the Tapajós center of endemism (between the Tapajós and Xingu rivers); and *Neacomys xingu*, sp. nov., restricted to the Xingu center of endemism (between the Xingu and Araguaia/Tocantins rivers). The new species can be discriminated from other *Neacomys* species by the morphology of the nasal bones, zygomatic plate, interorbital region, subsquamosal fenestra, paraoccipital process, incisive foramina, auditory bullae, anterocone and anteroloph of the first upper molar, carotid circulation pattern, and karyotype. Our results substantially improve our understanding of the genus *Neacomys* by providing morphological, morphometric, and novel molecular insights about these poorly known rodents and demonstrate that the diversity of small Amazonian mammals is still poorly known, even in the relatively accessible southeastern part of the biome.

INTRODUCTION

Species of *Neacomys* Thomas, 1900, are small (<42 g) Neotropical rodents belonging to the tribe Oryzomyini in the cricetid subfamily Sigmodontinae. Commonly known as spiny mice or bristly mice, they occur in forested habitats of Central and South America, from eastern Panama to central Bolivia and central/western Brazil (Weksler and Bonvicino, 2015). Fourteen nominal taxa are referred to the genus, of which 12 are currently recognized as valid: *N. amoenus* Thomas, 1903; *N. dubosti* Voss et al., 2001; *N. guianae* Thomas, 1905; *N. macedoruizi* Sánchez-Vendizú et al., 2018; *N. minutus* Patton et al., 2000; *N. musseri* Patton et al., 2000; *N. paracou* Voss et al., 2001; *N. pictus* Goldman, 1912; *N. rosalindae* Sánchez-Vendizú et al., 2018; *N. spinosus* (Thomas, 1882); *N. tenuipes* Thomas, 1900; and *N. vargasllosai* Hurtado and Pacheco, 2017. The nominal taxon *pusillus* Allen, 1912, has been considered a junior synonym of *N. tenuipes* (see Weksler and Bonvicino, 2015), and the nominal taxon *carceleni* Hershkovitz, 1940, is currently considered to be a valid subspecies of *N. amoenus* (see Hurtado and Pacheco, 2017).

In their monographic study of the small mammals from the Juruá River, Brazil, a right-bank tributary of the Amazon River, Patton et al. (2000) estimated the phylogenetic affinities of local populations of *Neacomys* and assessed their taxonomic status. Based on sequence data from one mitochondrial gene (cytochrome *b*), linear body measurements, and discrete morphological data, these authors revealed the existence of several previously unrecognized clades within the genus. In addition to providing the first gene tree for the group, these authors documented high levels of genetic differentiation among several morphologically diagnosable lineages. Based on these results, Patton et al. (2000) described two new species from western Amazonia and suggested the existence of an undescribed taxon from eastern Amazonia, which they referred to as "*Neacomys* sp. clade 7."

In a monograph on the mammals of Paracou, French Guiana, Voss et al. (2001) assessed the taxonomic status of local samples of *Neacomys*, provided an emended morphological diagnosis for the genus, and described two new sympatric species for the Guiana Region. More

recently, three new species have been described from western Amazonia (eastern Peru) based on molecular, morphological, and karyotypic data (Hurtado and Pacheco, 2017; Sánchez-Vendizú et al., 2018).

Cytogenetic studies have also indicated the existence of undescribed species of *Neacomys* in the eastern Amazon of Brazil. Silva et al. (2015) reported new karyotypes for specimens from Marajó Island and from Marabá, both in eastern Pará state, and Oliveira da Silva et al. (2017) described two additional new karyotypes associated with specimens from the right and left banks of the Tapajós River. By using comparative chromosome painting analyses, Oliveira da Silva et al. (2019) described yet another new karyotype for specimens from Santa Bárbara (in eastern Pará) and suggested that this and the other cytotypes previously reported by Silva et al. (2015) and Oliveira da Silva et al. (2017) could represent new species.

In view of the seven new species described in the past 20 years (Patton et al., 2000; Voss et al., 2001; Hurtado and Pacheco, 2017; and Sánchez-Vendizú et al., 2018), and the possible existence of undescribed taxa as suggested by molecular and cytogenetic studies (e.g., Patton et al., 2000; Hurtado and Pacheco, 2017; Sánchez-Vendizú et al., 2018; Oliveira da Silva et al., 2019), it is clear that *Neacomys* is much more diverse than had been assumed by mid-20th century authors (e.g., Cabrera, 1961). However, despite the geographically restricted studies mentioned earlier, no comprehensive taxonomic revision has ever been undertaken for the genus. As a result, the systematics of *Neacomys* remains a work in progress, and little is yet known about the geographic limits of the species currently recognized as valid; additionally, phylogenetic relationships, especially of the unnamed forms in the eastern Amazon, remain obscure. In fact, the need for a critical taxonomic reevaluation of the genus is widely recognized (Woodman et al., 1991; Voss et al., 2001; Musser and Carleton, 2005; Catzeflis and Tilak, 2009; Weksler and Bonvicino, 2015; Hurtado and Pacheco, 2017; Sánchez-Vendizú et al., 2018).

In this report, we review the alpha taxonomy of *Neacomys* from southeastern Amazonia and provide preliminary hypotheses about their phylogenetic relationships. Based on phylogenetic analyses of the mitochondrial cytochrome *b* gene, together with external and craniodental characters, we define the species limits of the populations occurring in the southeastern parts of Brazilian Amazonia. In total, we recognize four species of *Neacomys* in southeastern Amazonia, three of them herein described as new. Our work represents a first step toward a thorough systematic review, offering novel data to enlighten future biogeographic, taxonomic, and evolutionary studies of this neglected group of rodents.

Materials and Methods

Source of Material: We analyzed a total of 174 specimens (skulls, skins, and entire fluid-preserved specimens), including name-bearing types and other important material from most of the distributional range of *Neacomys* (table 1; appendix 1). This examined material, as well as unexamined vouchers for specimens with analyzed molecular sequences, is deposited in the following collections (abbreviations in parentheses): American Museum of Natural History, New York (AMNH); Natural History Museum, London (BMNH); Carnegie Museum,

TABLE 1. List of sequenced specimens of *Neacomys* included in phylogenetic analyses of cytochrome *b*. (Voucher material marked with asterisks (*) was examined by the authors.)

Taxon	Voucher	GenBank	Locality	Source
amoenus amoenus	UFMT 1669*	MT462078	Brazil: Mato Grosso	This study
amoenus amoenus	UFMT 1659*	MT462079	Brazil: Mato Grosso	This study
amoenus amoenus	UFMT 1367*	MT462080	Brazil: Mato Grosso	This study
amoenus amoenus	UFMT 1374*	MT462081	Brazil: Mato Grosso	This study
amoenus amoenus	UFMT 1373*	MT462082	Brazil: Mato Grosso	This study
amoenus amoenus	UFMT 1370*	MT462083	Brazil: Mato Grosso	This study
amoenus amoenus	MAS NB 46 *	MT462084	Brazil: Rondonia	This study
amoenus amoenus	MSA FM 02*	MT462085	Brazil: Rondonia	This study
amoenus amoenus	INPA 3059*	MT462015	Brazil: Acre	This study
amoenus amoenus	INPA 3064*	MT462016	Brazil: Amazonas	This study
amoenus amoenus	INPA 3063*	MT462017	Brazil: Amazonas	This study
amoenus amoenus	UFMT 3382*	MT462086	Brazil: Mato Grosso	This study
amoenus amoenus	UFMT 3380*	MT462087	Brazil: Mato Grosso	This study
amoenus amoenus	MVZ 155015*	KX792049	Peru: Amazonas	Hurtado and Pacheco, 2017
amoenus amoenus	MVZ 190634*	MT462019	Brazil: Amazonas	Patton et al., 2000 [k]
amoenus amoenus	MVZ 190635*	MT462020	Brazil: Amazonas	Patton et al., 2000 [k]
amoenus amoenus	INPA 3057*	MT462021	Brazil: Amazonas	This study
amoenus amoenus	MVZ 190372*	KX792040	Brazil: Amazonas	Patton et al., 2000
amoenus amoenus	USNM 588096	KX792042	Perú: Cusco	Hurtado and Pacheco, 2017
amoenus amoenus	USNM 588051	KX792041	Perú: Cusco	Hurtado and Pacheco, 2017
amoenus amoenus	USNM 584543	KX792022	Bolivia: Santa Cruz	Patton et al., 2000
amoenus amoenus	USNM 584544	MT462022	Bolivia: Santa Cruz	Patton et al., 2000 [k]
amoenus amoenus	INPA 3058*	KY859734	Brazil: Acre	Sánchez-Vendizú et al., 2018
amoenus amoenus	INPA 3060*	KX792032	Brazil: Acre	Hurtado and Pacheco, 2017
amoenus amoenus	INPA 3062*	KX792033	Brazil: Acre	Hurtado and Pacheco, 2017
amoenus amoenus	UFMT 1763*	MT462076	Brazil: Mato Grosso	This study
amoenus amoenus	UFMT 1757*	MT462077	Brazil: Mato Grosso	This study
amoenus carceleni	ROM 104474	KX792045	Ecuador: Napo	Hurtado and Pacheco, 2017
amoenus carceleni	ROM 105278	KX792046	Ecuador: Napo	Hurtado and Pacheco, 2017
amoenus carceleni	ROM 105282	KY859738	Ecuador: Napo	Sánchez-Vendizú et al., 2018
amoenus carceleni	ROM 105290	KX792047	Ecuador: Napo	Hurtado and Pacheco, 2017
amoenus carceleni	ROM 105264	MT462018	Ecuador: Napo	Patton et al., 2000 [k]
amoenus carceleni	USNM 574567	KX792048	Ecuador: Pastaza	Hurtado and Pacheco, 2017
dubosti	CN 240 *	MT462036	Brazil: Pará	This study
dubosti	CM 76846 [a]	FM210781	Suriname: Nickerie	Catzeflis et al., 2009
dubosti	V-1134	FM210773	France: French Guiana	Catzeflis et al., 2009
guianae	CM 76847*	FM210778	Suriname: Nickeri	Catzeflis et al., 2009

Taxon	Voucher	GenBank	Locality	Source
guianae	INPA 7102*	MT462037	Brazil: Amazonas	This study
guianae	INPA 7100*	MT462038	Brazil: Amazonas	This study
macedoruizi	MUSM 45054[b]	KY859731	Peru: Huánuco	Sánchez-Vendizú et al., 2018
macedoruizi	MUSM 45053 [c]	KY859732	Peru: Huánuco	Sánchez-Vendizú et al., 2018
marajoara	MPEG40440	KX752075	Brazil: Pará	Oliveira da Silva et al., 2017
marajoara	MPEG 40443	KX752072	Brazil: Pará	Oliveira da Silva et al., 2017
marajoara	MPEG 40441	MT462067	Brazil: Pará	This study
marajoara	MPEG 40446	KX752080	Brazil: Pará	Oliveira da Silva et al., 2017
marajoara	MPEG 40435	MT462068	Brazil: Pará	This study
marajoara	MPEG 40434	MT462069	Brazil: Pará	This study
marajoara	MPEG 40432 [d]	MT462070	Brazil: Pará	This study
marajoara	MPEG 40431	MT462071	Brazil: Pará	This study
marajoara	MPEG 40429	MT462072	Brazil: Pará	This study
minutus "downriver"	SISPUR 159*	MT462039	Brazil: Amazonas	This study
minutus "downriver"	SISPUR 151*	MT462040	Brazil: Amazonas	This study
minutus "downriver"	INPA 5392*	MT462023	Brazil: Amazonas	This study
minutus "downriver"	INPA 5387*	MT462007	Brazil: Amazonas	This study
minutus "downriver"	INPA 3048*	MT462008	Brazil: Amazonas	This study
minutus "downriver"	INPA 3049*	MT462009	Brazil: Amazonas	This study
minutus "downriver"	EE 110*	MT462041	Brazil: Amazonas	This study
minutus "downriver"	MVZ 190360	KY859739	Brazil: Amazonas	Patton et al., 2000
minutus "downriver"	MVZ 190361	KX792069	Brazil: Amazonas	Patton et al., 2000
minutus "downriver"	MVZ 191209	KX792072	Brazil: Amazonas	Patton et al., 2000
minutus "downriver"	MVZ 190359	KX792068	Brazil: Amazonas	Patton et al., 2000
minutus "downriver"	MVZ 190363	KX792071	Brazil: Amazonas	Patton et al., 2000
minutus "downriver"	INPA 3051*	KX792065	Brazil: Amazonas	Hurtado and Pacheco, 2017
minutus "downriver"	INPA 3047*	KX792063	Brazil: Amazonas	Hurtado and Pacheco, 2017
minutus "downriver"	INPA 2689* [e]	MT462010	Brazil: Amazonas	This study
minutus "upriver"	INPA 3055*	MT462011	Brazil: Amazonas	This study
minutus "upriver"	INPA 3053*	MT462012	Brazil: Amazonas	This study
minutus "upriver"	MVZ 190358	U58392	Brazil: Amazonas	Sánchez-Vendizú et al., 2018
minutus "upriver"	INPA 3050*	KX792064	Brazil: Amazonas	Sánchez-Vendizú et al., 2018
minutus "upriver"	MVZ 190362	KX792070	Brazil: Amazonas	Sánchez-Vendizú et al., 2018
minutus "upriver"	INPA 3891*	KX792066	Brazil: Amazonas	Sánchez-Vendizú et al., 2018
minutus "upriver"	INPA 3056*	KY886326	Brazil: Amazonas	Sánchez-Vendizú et al., 2018
musseri	MVZ 171487	KX792074	Perú: Cusco	Hurtado and Pacheco, 2017
musseri	MVZ 171488	KY859742	Perú: Cusco	Patton et al., 2000
musseri	INPA 3046* [f]	U58392	Brazil: Acre	Hurtado and Pacheco, 2017

Taxon	Voucher	GenBank	Locality	Source
paracou	CN 279*	MT462042	Brazil: Pará	This study
paracou	CN 263*	MT462043	Brazil: Pará	This study
paracou	MPEG 40080*	MT462044	Brazil: Pará	This study
paracou	MPEG 40078*	MT462045	Brazil: Pará	This study
paracou	CN 129 *	MT462046	Brazil: Pará	This study
paracou	MPEG 40000*	MT462047	Brazil: Pará	This study
paracou	MPEG 39998*	MT462048	Brazil: Pará	This study
paracou	INPA 7089 *	MT462049	Brazil: Amazonas	This study
paracou	INPA 7138 *	MT462050	Brazil: Amazonas	This study
paracou	ROM 114325*	FM210782	Surinam: Brokopondo	Catzeflis et al., 2009
paracou	ROM 114315*	FM210767	Surinam: Brokopondo	Catzeflis et al., 2009
rosalindae	ROM 104560	KX792050	Ecuador: Napo	Hurtado and Pacheco, 2017
rosalindae	ROM 105265	KX792051	Ecuador: Napo	Hurtado and Pacheco, 2017
rosalindae	ROM 105314	KX792052	Ecuador: Napo	Hurtado and Pacheco, 2017
rosalindae	ROM 105315	KX792053	Ecuador: Napo	Hurtado and Pacheco, 2017
rosalindae	MVZ 153530	KX792054	Peru: Amazonas	Hurtado and Pacheco, 2017
rosalindae	MVZ 155299	KY859730	Peru: Amazonas	Sánchez-Vendizú et al., 2018
rosalindae	KU 158172	KX792055	Peru: Loreto	Hurtado and Pacheco, 2017
species 1	INPA 4190	KX792061	Brazil: Amazonas	Hurtado and Pacheco, 2017
species 1	INPA 4191	KX792062	Brazil: Amazonas	Hurtado and Pacheco, 2017
species 1	INPA 4189	KX792059	Brazil: Amazonas	Hurtado and Pacheco, 2017
species 1	INPA 4192	KX792060	Brazil: Amazonas	Hurtado and Pacheco, 2017
species 1	MPEG 45483	MT462051	Brazil: Amazonas	This study
species 2	MPEG 42838	MT462052	Brazil: Pará	This study
species 2	JUR 82	MT462053	Brazil: Pará	This study
species 2	JUR 19	MT462054	Brazil: Pará	This study
species 2	UFPA 1227	MT462034	Brazil: Pará	This study
species 2	UFPA 1530	MT462035	Brazil: Pará	This study
species 2	UFPA 1413	MT462055	Brazil: Pará	This study
species 2	JUR 042	MT462056	Brazil: Pará	This study
species 2	MPEG 42901	MT462057	Brazil: Pará	This study
spinosus	MUSM 36924	KX258228	Peru: Amazonas	Hurtado and Pacheco, 2017
tenuipes	BMNH 1899.10.3.34*[g]	KX792081	Colombia: Cundinamarca	Patton et al., 2000
vargasllosai	MVZ 172650	KX792082	Peru: Puno	Hurtado and Pacheco, 2017
vargasllosai	MVZ 172654	MT462013	Peru: Puno	Patton et al., 2000 [k]
vargasllosai	MVZ 172655	MT462014	Peru: Puno	Patton et al., 2000 [k]
vossi	UFPA 1277	MT462024	Brazil: Pará	This study
vossi	UFPA 1284	MT462025	Brazil: Pará	This study

Taxon	Voucher	GenBank	Locality	Source
vossi	UFPA 1647	MT462026	Brazil: Pará	This study
vossi	UFPA 1467	MT462027	Brazil: Pará	This study
vossi	UFPA 1583 [h]	MT462028	Brazil: Pará	This study
vossi	UFPA 1736	MT462073	Brazil: Pará	This study
vossi	UFPA 1577	MT462029	Brazil: Pará	This study
vossi	UFPA 1691	MT462030	Brazil: Pará	This study
vossi	UFPA 1520	MT462031	Brazil: Pará	This study
vossi	UFPA 1444	MT462074	Brazil: Pará	This study
vossi	UFPA 1391	MT462075	Brazil: Pará	This study
vossi	UFPA 1654	MT462032	Brazil: Pará	This study
vossi	UFPA 1487	MT462033	Brazil: Pará	This study
xingu	UFMT 1275	MT462058	Brazil: Pará	This study
xingu	UFMT 1273	MT462059	Brazil: Pará	This study
xingu	UFMT 1268 [i]	MT462060	Brazil: Pará	This study
xingu	MPEG 41805	MT462061	Brazil: Pará	This study
xingu	MPEG 42019	MT462062	Brazil: Pará	This study
xingu	MPEG 41804	KX752073	Brazil: Pará	Oliveira da Silva et al., 2017
xingu	MPEG 41996	MT462063	Brazil: Pará	This study
xingu	PSA 69	MT462064	Brazil: Pará	This study
xingu	MPEG 41991	MT462065	Brazil: Pará	This study
xingu	PSA 46	MT462066	Brazil: Pará	This study
xingu	USNM 549553 [j]	KX792080	Brazil: Pará	Hurtado and Pacheco, 2017

[a] Paratype of *Neacomys dubosti*.
[b] Paratype of *Neacomys macedoruizi*.
[c] Holotype of *Neacomys macedoruizi*.
[d] Holotype of *Neacomys marajoara*.
[e] Holotype of *Neacomys minutus*.
[f] Paratype of *Neacomys musseri*.
[g] Holotype of *Neacomys tenuipes*.
[h] Holotype of *Neacomys vossi*.
[i] Holotype of *Neacomys xingu*.
[j] *Neacomys* "clade 7" of Patton et al., 2000.
[k] Unpublished data from Patton et al., 2000.

Pittsburgh (CM); Instituto Nacional de Pesquisas da Amazônia, Manaus (INPA); Pontifícia Universidade Católica de Minas Gerais, Belo Horizonte (MCN-M); University of Kansas Biodiversity Research Center, Lawrence (KU); Muséum d'Histoire Naturelle de la Ville de Genève, Geneva (MHNG), Muséum National d'Histoire Naturelle, Paris (MNHN); Museu Paraense Emílio Goeldi, Belém (MPEG); Museo de Historia Natural de la Universidad Nacional Mayor de San Marcos, Lima (MUSM); Museum of Vertebrate Zoology, University of California, Berkeley (MVZ); Royal Ontario Museum, Toronto (ROM); Coleção Zoológica da Universidade Federal de Mato Grosso, Cuiabá (UFMT); Universidade Federal do Pará, Belém (UFPA); and National Museum of Natural History, Smithsonian Institution, Washington (USNM). Specimens with field numbers prefixed by CN, JUR, and PSA are currently held at the MPEG and by MAS NB, MSA FM, EE, and SISPUR are currently held at INPA. Those specimens will be deposited in the aforementioned collections.

Collecting Localities: Geographic data for collection localities were obtained from specimen tags. For specimens unaccompanied by geographic coordinates, we referred to Paynter and Traylor (1991), Paynter (1993), Prado and Percequillo (2013), Gardner (2008), and Patton et al. (2015) to obtain this information.

Molecular Analyses

Taxon Sampling: We obtained partial sequences (801 bp) of the mitochondrial cytochrome *b* gene (*Cytb*) from 75 Amazonian specimens of *Neacomys*. These new sequences are deposited in GenBank with accession numbers MT462007–MT462087. In addition, we downloaded 54 ingroup (*Neacomys*) sequences from GenBank and another six unpublished sequences from Patton et al.'s (2000) dataset (table 1). In total, our ingroup dataset includes all currently recognized species in the genus, with the sole exception of *N. pictus* (for which no sequence data are available). Among other nomenclaturally important sequences, we analyzed *Cytb* data from the holotypes of *N. minutus* (INPA 2689) and *N. tenuipes* (BMNH 1899.10.3.34), a paratype of *N. musseri* (INPA 3046), and the holotype (MUSM 45053) and a paratype (MUSM 45054) of *N. macedoruizi*.

We obtained sequences of the following outgroup taxa from Genbank (accession numbers in parentheses): *Thomasomys baeops* (DQ914654), *Hylaeamys megacephalus* (KF815441), *Oligoryzomys microtis* (OMU58381), *Scolomys ucayalensis* (EU579518), *Oreoryzomys balneator* (EU579510), and *Microryzomys minutus* (AF108698). The *T. baeops* sequence was used to root the trees in our phylogenetic analyses. Outgroup taxa were chosen based on the phylogenies of Weksler (2003), Weksler (2006), and Percequillo et al. (2011).

Laboratory Procedures: We extracted genomic DNA from ethanol-preserved tissues using the salt-extraction method (Aljanabi and Martinez, 1997). The *Cytb* gene was PCR-amplified using primers developed by Smith and Patton (1993): MVZ05 (5′-CGAAGCTTGATATGAAAAACCATCGTTG-3′) and MVZ16 (5′AAATAGGAARTATCAYTCTGGTTTRAT-3′). Each PCR reaction contained 2.5 μL of 10x buffer, 1.0 μL of $MgCl_2$ (50 mM), 1.25 μL of dNTP mix (1.25 mM for each nucleotide), 1 μL of each primer (10 mM), 0.2 μL of Ludwig Biotechnolgia Taq DNA Polymerase (5 μ/μL), 1 μL of DNA template, and water to a final volume of

25 μL. For some difficult templates, concentrations of reagents were adjusted to increase PCR success. PCR conditions used a preheating step of initial denaturation at 94° C for 3–5 min, followed by 35 cycles at 94° C for 30 sec, 49° C for 45 sec, and 72° C for 1 min and 45 sec, and a final extension at 72° C for 5–7 min. PCR products were cleaned using Exonuclease I and shrimp alkaline phosphatase (Fermentas), and sequenced using an ABI 3130xl Genetic Analyzer (Life Technologies).

Molecular Data Analyses: We aligned sequences with Clustal W (Thompson et al., 1994) using default parameters. Phylogenetic analyses were performed using maximum likelihood (ML) and Bayesian inference (BI). We coded all missing bases as unknown ("?") prior to phylogenetic analyses. PartitionFinder ver. 2.1.1 (Lanfear et al., 2017)—which heavily relies on PhyML (Guindon et al., 2010)—was employed to select both the most suitable partition scheme and the best-fit model of nucleotide substitution for each data subset. The Akaike Information Criterion (AIC) was used to select the best-fit models; only models that could be applied in MrBayes were considered, and the "greedy" algorithm was implemented.

In order to find the best topology according to the ML optimality criterion, we conducted an analysis with 50 independent searches in GARLI 2.01 (Zwickl, 2006) using default settings. Maximum-likelihood bootstrap analysis was also carried out in GARLI 2.01 and implemented in the CIPRES Science Gateway (Miller et al., 2010) using 100 pseudoreplicated data matrices with 10 searches performed on each. The Bayesian analysis was conducted using the Markov Chain Monte Carlo (MCMC) sampling approach in MrBayes v. 3.2.3 (Huelsenbeck and Ronquist, 2001; Ronquist and Huelsenbeck, 2003; Altekar et al., 2004; Ronquist et al., 2012) and was also implemented through the CIPRES Science Gateway. The search started with a random tree and consisted of one cold chain and three heated chains. The Markov chains were run for 100,000,000 generations, and trees were sampled every 1000 generations. Default values were kept for the "relburnin" and "burninfrac" options in MrBayes; hence, the first 25,000,000 generations (i.e., 250,000 trees or 25%) were discarded as burn-in, and posterior probability estimates of all model parameters were based on the remaining (750,000) trees.

We calculated average pairwise genetic distances within and between groups using the uncorrected (p-distance) option in MEGA 6 (Tamura et al., 2011). Uncorrected distances were chosen to allow comparison with divergence estimates reported in previous studies of *Neacomys* (e.g., by Hurtado and Pacheco, 2017; Sánchez-Vendizú et al., 2018).

Morphological and Morphometric Analyses

Morphology: We examined the following external and craniodental characters for taxonomic variation: dorsal and ventral pelage color, tail color, morphology of the palate, carotid circulation type, features of the auditory bullae, and dental morphology. We made comparisons predominantly among specimens of the same age class to avoid conflating ontogenetic variation with taxonomic differences. Nomenclature for external and craniodental morphology follows Voss (1988), Patton et al. (2000), Voss et al. (2001), Weksler (2006), Hurtado and Pacheco (2017), and Sánchez-Vendizú et al. (2018).

Age Criteria: In order to distinguish ontogenetic from taxonomic variation, we grouped specimens into age classes based on patterns of molar eruption and degree of tooth wear (fig. 1), using the criteria defined by Voss (1991):

Age class 1 M3 incompletely erupted or unworn;
Age class 2 M3 fully erupted and exhibiting slight to moderate wear (some dentine exposed), but the occlusal surface still tubercular (the paracone raised and prominent), not flat;
Age class 3 M3 well worn, the occlusal surface flat or concave; M1–2 tubercular (the major cusps all separate and prominent); anteroloph of M2 distinct, not fused with paracone;
Age class 4 M3 flat or concave; M1–2 with cusps worn almost or quite flat but not below widest part of crown; anteroloph of M2 obliterated, fused with paracone;
Age class 5 M1–3 all worn flat or concave, below widest part of crowns; most details of occlusal topography obliterated.

Hereafter, we refer to specimens in age class 1 as "juveniles," specimens in age classes 2–4 as "adults," and specimens in age class 5 as "old adults."

Measurements: We obtained 21 craniodental measurements (in millimeters, mm) that have been previously used in taxonomic studies of Neotropical cricetids (Voss, 1988; Patton et al., 2000; Voss et al., 2001; Flores et al., 2010). The following dimensions were measured with digital calipers to the nearest 0.01 mm while skulls were examined at low magnification under a stereomicroscope:

BH Braincase height, measured in the midline from the basisphenoid-basioccipital suture on the ventral surface of the skull to the frontal-parietal suture on the dorsal surface;
BI Breadth of incisive foramen, the greatest transverse dimension across both incisive foramina;
BM1 Breadth of M1, greatest crown breadth of the first upper molar (M1);
BPR Breadth of palate at rostrum, measured between most posterior lower edges of the left and right infraorbital foramina on the ventral side of skull;
BZP Breadth of zygomatic plate, least distance between the anterior and posterior edges of the zygomatic plate;
BB Bullar breadth, distance between anterior opening of carotid foramen to ectotimpanic dorsal process;
CIL Condylo-incisive length, from the greater curvature of one upper incisor to the articular surface of the condyle on the same side;
LCIB Least condyloid-incisor breadth, greatest distance from the lower incisor base to the posterior margin of the condyloid process on the same side of the mandible;
LIB Least interorbital breadth, least distance across the frontal bones between the orbital fossae;
LD Length of diastema, from the crown of M1 to the lesser curvature of the incisor on the same side;
LIF Length of incisive foramen, greatest anterior-posterior dimension of one incisive foramen;

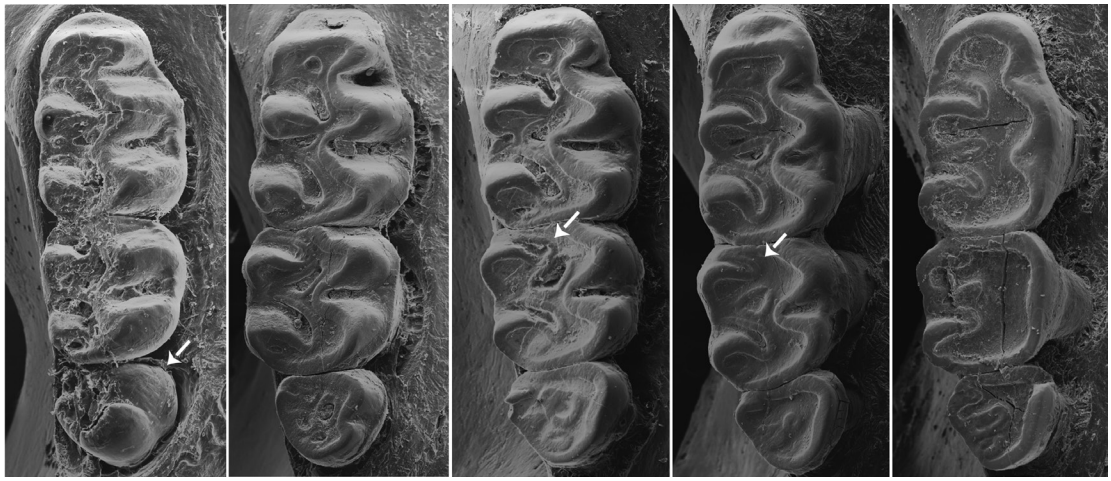

FIG. 1. SEM images of molar toothwear age classes of *Neacomys amoenus* used in this study (based on Voss, 1991). From left to right: age class 1 (UFMT 4050), age class 2 (UFMT 1758), age class 3 (UFMT 1760), age class 4 (UFMT 1759), and age class 5 (UFMT 915). Arrows indicate the incompletely erupted M3 in age class 1, the distinct M2 anteroloph (not fused with the paracone) in age class 3, and the obliterated M2 anteroloph (fused with the paracone) in age class 4.

LLD Length of lower diastema, from the crown of m1 to the lesser curvature of the incisor on the same side of the mandible;

LLM Length of lower molars, crown length from m1 to m3;

LM Length of molars, crown length from M1 to M3;

LN Length of nasals, greatest anterior-posterior dimension of one nasal bone;

LPB Length of palatal bridge, from the posterior margin of the upper incisors to the anterior margin of the mesopterygoid fossa;

MB Mastoid breadth, distance across the cranium at the mastoid processes;

OL Orbital length, internal distance between the anterior and posterior margins of the right or the left orbit;

RB Rostral breadth, distance across the outside margins of the left and right nasolacrimal capsule;

RL Rostral length, diagonal measurement taken from the anterior margin of the orbit to the anterior margin of the nasal bone on the same side;

ZB Zygomatic breadth, greatest transverse dimension across the squamosal zygomatic processes.

In addition to these craniodental measurements, we transcribed five external measurements (in mm) taken in the field by collectors and recorded on specimen labels: total length (TL); length of head and body (HBL); length of tail (LT); length of hind foot (HF); and length of ear (Ear). We also transcribed weight (in grams, g) as recorded by collectors.

Statistical Analyses: We calculated standard descriptive univariate statistics for all external and craniodental measurements. In order to minimize potentially confounding ontogenetic variation, we included only adult and old adult specimens (age classes 2–5) in these analyses.

Principal component analyses (PCA) were conducted to assess whether morphometric data are congruent with results from the molecular analyses, qualitative morphological comparisons, and previously published karyotypic studies. For PCA, measurements were log-transformed and principal components were extracted from the variance-covariance matrix. Statistical analyses were performed using SPSS 22.0 for Windows.

RESULTS

Molecular Analyses

The *Cytb* gene fragment we sequenced was 801 base pairs long and included 470 conserved sites, 331 variable sites, and 287 parsimony-informative sites. Monophyly of *Neacomys* was recovered with strong support from our Bayesian analysis (Bayesian posterior probability [BPP] = 0.97); whereas our ML analysis provided only marginal support (bootstrap support [BS] = 51%) for generic monophyly (fig. 2A–C).

The gene trees obtained from our Bayesian and ML analyses both recovered 17 distinct lineages of *Neacomys*, 11 of which could be associated with taxa that are currently recognized as valid species: *N. dubosti*, *N. guianae*, *N. minutus*, *N. musseri*, *N. paracou*, *N. spinosus*, *N. rosalindae*, *N. macedoruizi*, *N. amoenus*, *N. vargasllosai*, and *N. tenuipes*. Among the remaining six lineages, three are formally described in this report (*N. vossi*, *N. xingu*, and *N. marajoara*) and three others are referred to by informal nomenclature: *N. minutus* "upriver" and *N. minutus* "downriver" (after Patton et al., 2000), *Neacomys* "sp. 1," and *Neacomys* "sp. 2." All these lineages received BPP support values ≥ 0.96, except for *N. minutus* "downriver" (BPP = 0.82). All undescribed lineages also had bootstrap values ≥ 94%, except for *N. xingu* and *N. marajoara* (with bootstrap values of 58% and 62%, respectively; fig. 2B). Mean interspecific genetic distances ranged from 3.9% (between *N. marajoara* and *N. xingu*) to 15.58% (between *N. paracou* and *N. musseri*; table 2), whereas intragroup divergences ranged from 0% in *N. macedoruizi* (two sequences from one locality) and *N. vargasllosai* (three sequences from one locality) to 1.88% in *N. amoenus* (34 sequences from 16 localities).

The only relationship that differs between our BI and ML topologies is the position of *N. tenuipes*, which is sister to a negligibly supported clade containing *N. minutus*, *N. macedoruizi*, *N. rosalindae*, *N. musseri*, *Neacomys* sp. 1, and *N. guianae* in the BI tree. By contrast, *N. tenuipes* is sister to a negligibly supported clade containing *N. dubosti*, *N. marajoara*, *Neacomys* sp. 2, *N. vossi*, and *N. xingu* in the ML tree (appendix 2).

Based on the BI topology, and for the purposes of this report, we recognize four groups of species within *Neacomys*. Two of these groups correspond to the Paracou and Spinosus groups (fig. 2C) of Hurtado and Pacheco (2017), whereas the Tenuipes Group (fig. 2A) of Hurtado and Pacheco (2017) was recovered as two monophyletic groups in our analysis. Herein we restrict the Tenuipes Group to *N. tenuipes*, *N. guianae*, *Neacomys* sp. 1, *N. musseri*, *N. rosalindae*, *N. macedoruizi*, and *N. minutus*; additionally, we recognize a Dubosti Group for *N. dubosti*, *Neacomys* sp. 2, and the three new species described in this report (*N. marajoara*, *N. xingu*, and *N. vossi*).

TABLE 2. Uncorrected average pairwise genetic distances (percent sequence divergence) within and among species of *Neacomys*.

		1	2	3	4	5	6	7	8	9	10	11	12	13	14	15	16	17
1	tenuipes	—																
2	*rosalindae*	8.4	**1.3**															
3	*guianae*	8.0	11.3	**0.9**														
4	species 1	8.8	10.6	7.5	**0.6**													
5	*minutus* "upriver"	10.3	10.6	12.3	12.5	**0.4**												
6	*macedoruizi*	9.0	10.2	12.3	12.1	4.7	—											
7	*minutus* "downriver"	12.0	11.4	12.4	12.2	7.2	5.4	**1.7**										
8	*musseri*	9.8	10.8	13.8	13.0	12.3	12.2	11.2	**1.5**									
9	*dubosti*	13.9	11.5	13.1	12.0	14.9	12.8	12.9	13.5	**0.7**								
10	species 2	15.6	12.9	14.1	11.3	13.7	13.3	12.1	13.8	10.7	**0.4**							
11	*vossi*	12.3	12.5	13.5	11.3	13.0	13.0	13.4	14.2	10.2	7.5	**0.5**						
12	*xingu*	13.2	12.4	13.3	12.2	11.9	11.4	12.4	13.3	10.1	6.9	5.1	**0.3**					
13	*marajoara*	11.7	12.3	13.1	12.0	12.7	12.4	13.0	13.9	9.3	8.7	5.4	3.9	**0.4**				
14	*amoenus*	11.7	13.8	14.3	14.1	14.7	13.4	13.6	14.0	12.3	12.6	12.4	12.7	12.2	**1.9**			
15	*vargasllosai*	8.5	12.1	13.5	12.3	13.0	12.7	12.4	11.8	13.0	12.9	12.2	12.6	12.8	8.3	—		
16	*spinosus*	12.8	12.6	15.1	13.3	14.0	13.7	13.8	13.5	13.8	13.9	13.6	14.4	13.9	8.1	8.3	—	
17	*paracou*	12.6	14.2	15.0	13.5	15.1	14.3	14.4	15.6	15.0	15.1	14.6	14.4	13.5	14.7	13.2	14.0	**1.2**

Neacomys paracou (comprising the monotypic Paracou Group) was recovered as sister to the remaining species of *Neacomys* with strong Bayesian support, whereas the Spinosus Group was recovered as sister to the Dubosti and Tenuipes groups with strong Bayesian support. The sister-group relationship between the Dubosti and Tenuipes groups also received strong Bayesian support. Within the Spinosus Group, *N. vargasllosai* was recovered as sister to *N. spinosus* + *N. amoenus* with consistently strong support. Within the Dubosti Group, the sister-group relationship of *N. dubosti* to other group members in the nested clades (*N. marajoara* (*N. xingu* (*Neacomys* sp. 2 + *N. vossi*))) is also strongly supported. Lastly, with negligible support values, the Tenuipes Group includes *N. tenuipes* as sister to ((*N. guianae* + *Neacomys* sp. 1) ((*N. musseri* + *N. rosalindae*) ((*N. macedoruizi* + *N. minutus* "upriver") *N. minutus* "downriver"))). In general, *Cytb* provided satisfactory resolution of supraspecific phylogenetic relationships. However, among the new species described herein, the relationships of *N. xingu* and *N. vossi* had negligible support values.

Morphometric Analyses

Descriptive statistics for adult and old adult specimens of *Neacomys dubosti* and three new species from southeastern Amazonia are shown in table 3. In general, our results document univariate and multivariate morphometric overlap among all species in the Dubosti Group. In all pairwise multivariate analyses herein provided, the first principal components comprise only positive coefficient values, indicating that they are predominantly related to variation in skull size. Comparing *N. dubosti* with *N. marajoara,* the plot of first (PC1) and second principal components (PC2) shows that specimens of *N. dubosti* group at the higher extremity of the size axis (fig. 3A, appendix 3). The PC1 corresponds to 46.98% of the total variation and is strongly related to CIL and ZB while the PC2 corresponds to 12.62% of the total variation and is strongly related to LIF and LM. Similarly, *N. dubosti* tended to occupy the higher extremity of the size axis when compared to *N. vossi* (fig. 3B, appendix 3). In this analysis, PC1 corresponds to 47.22 % of the total variation and is strongly related to CIL and ZB, while the PC2 corresponds to 11.31% of the total variation and is strongly related to LIF and LCIB. By contrast, *N. dubosti* largely overlaps *N. xingu* in the morphospace (fig. 3C, appendix 3). In this analysis, the PC1 explains 35.58% of the total variation and is strongly related to CIL, LD and ZB, while the PC2 explains 13.33% and is strongly related to BH, LN, and LCIB.

When *N. marajoara* was compared with *N. vossi* (fig. 3D, appendix 3), the PC1 explained 28.97 % of the total variation, while the PC2 explained 15.48%. The specimens largely overlapped on both axes, and the measurements that most contributed for the variation were CIL, LIF, LN, RL, and ZB. By comparing *N. marajoara* and *N. xingu* (fig. 3E, appendix 3), the PC1 explained 41.20 % of the total variance, while the PC2 explained 12.35%. The latter species appeared at the higher extremity of the size axis, and the measurements with highest loadings were BZP, CIL, LN, RL, and ZB.

In the PCA including *N. vossi* and *N. xingu* (fig. 3F, appendix 3), the PC1 explained 41.13 % of the total variance, while the PC2 explained 10.94%. The latter species appeared at the higher extremity of the size axis, and the variables that better contributed for variation were CIL, LM, LN, RL, and ZB.

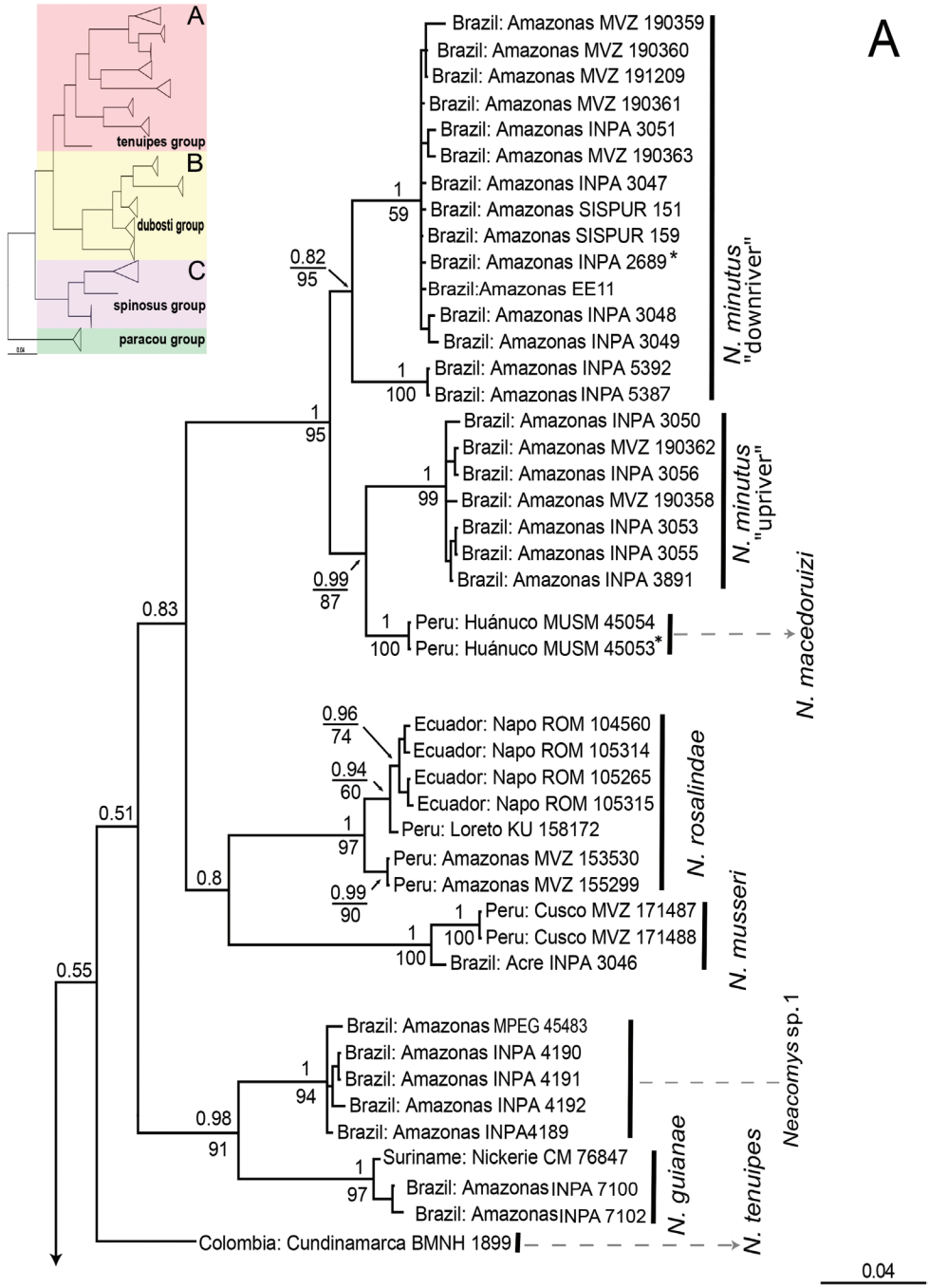

FIG. 2 A–C (*above and following two pages*). Bayesian phylogeny of *Neacomys* based on cytochrome *b* sequence data. Numbers represent Bayesian posterior probabilities (above) and ML bootstrap support (below) at nodes recovered by both analyses (bootstrap support for nodes only recovered by our ML analysis are shown in appendix 2). Only ML bootstrap support >50% is shown. Branch tips are labeled with geographic identifiers and voucher codes listed in table 1. Specimens marked with asterisks (*) indicate holotypes.

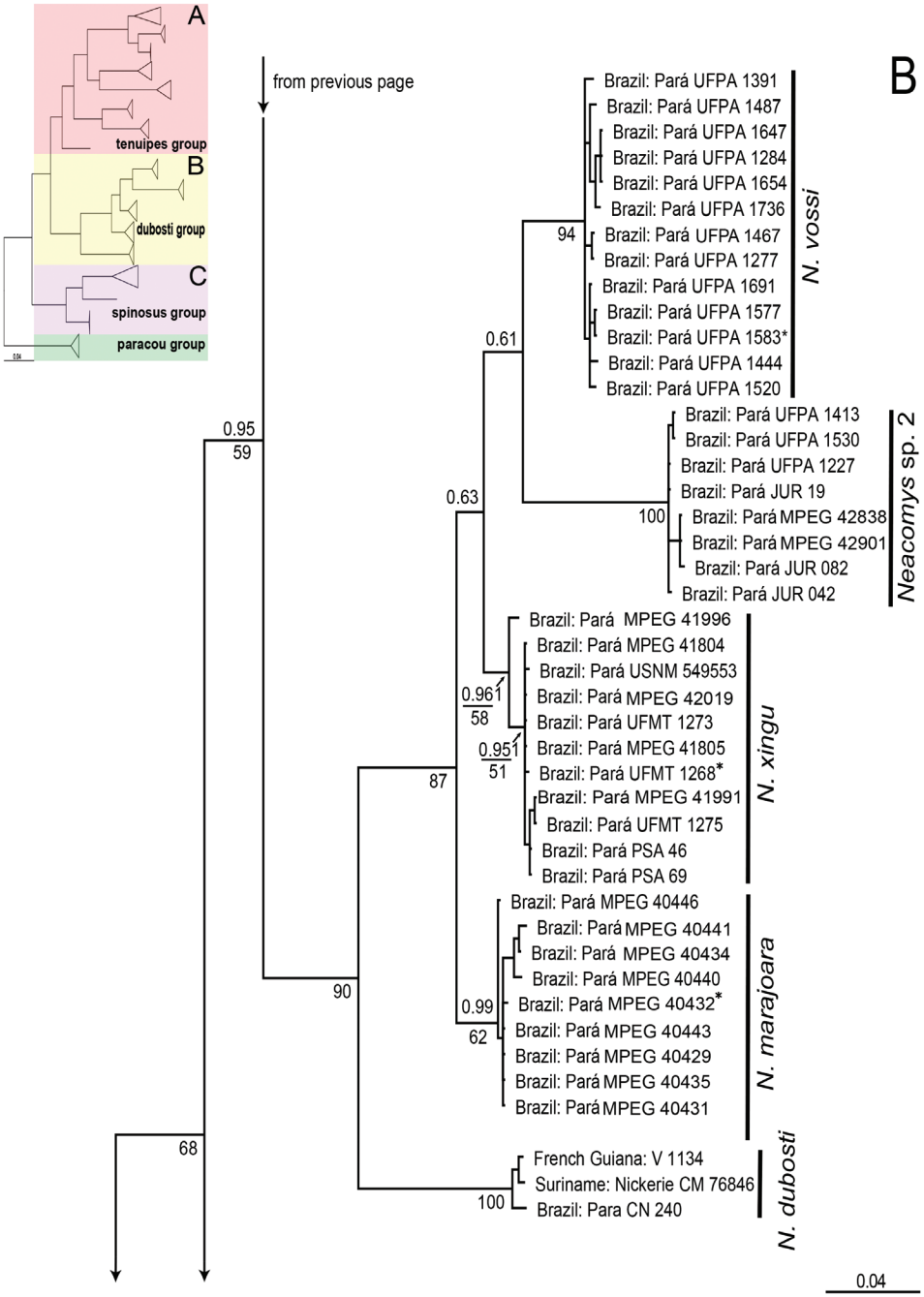
A
tenuipes group
B
dubosti group
C
spinosus group
paracou group
from previous page
B
Brazil: Pará UFPA 1391
Brazil: Pará UFPA 1487
Brazil: Pará UFPA 1647
Brazil: Pará UFPA 1284
Brazil: Pará UFPA 1654
Brazil: Pará UFPA 1736
Brazil: Pará UFPA 1467
Brazil: Pará UFPA 1277
Brazil: Pará UFPA 1691
Brazil: Pará UFPA 1577
Brazil: Pará UFPA 1583*
Brazil: Pará UFPA 1444
Brazil: Pará UFPA 1520
N. vossi
Brazil: Pará UFPA 1413
Brazil: Pará UFPA 1530
Brazil: Pará UFPA 1227
Brazil: Pará JUR 19
Brazil: Pará MPEG 42838
Brazil: Pará MPEG 42901
Brazil: Pará JUR 082
Brazil: Pará JUR 042
Neacomys sp. 2
Brazil: Pará MPEG 41996
Brazil: Pará MPEG 41804
Brazil: Pará USNM 549553
Brazil: Pará MPEG 42019
Brazil: Pará UFMT 1273
Brazil: Pará MPEG 41805
Brazil: Pará UFMT 1268*
Brazil: Pará MPEG 41991
Brazil: Pará UFMT 1275
Brazil: Pará PSA 46
Brazil: Pará PSA 69
N. xingu
Brazil: Pará MPEG 40446
Brazil: Pará MPEG 40441
Brazil: Pará MPEG 40434
Brazil: Pará MPEG 40440
Brazil: Pará MPEG 40432*
Brazil: Pará MPEG 40443
Brazil: Pará MPEG 40429
Brazil: Pará MPEG 40435
Brazil: Pará MPEG 40431
N. marajoara
French Guiana: V 1134
Suriname: Nickerie CM 76846
Brazil: Para CN 240
N. dubosti
0.95
59
0.61
94
0.63
100
0.961
58
0.951
51
87
90
0.99
62
68
100
0.04

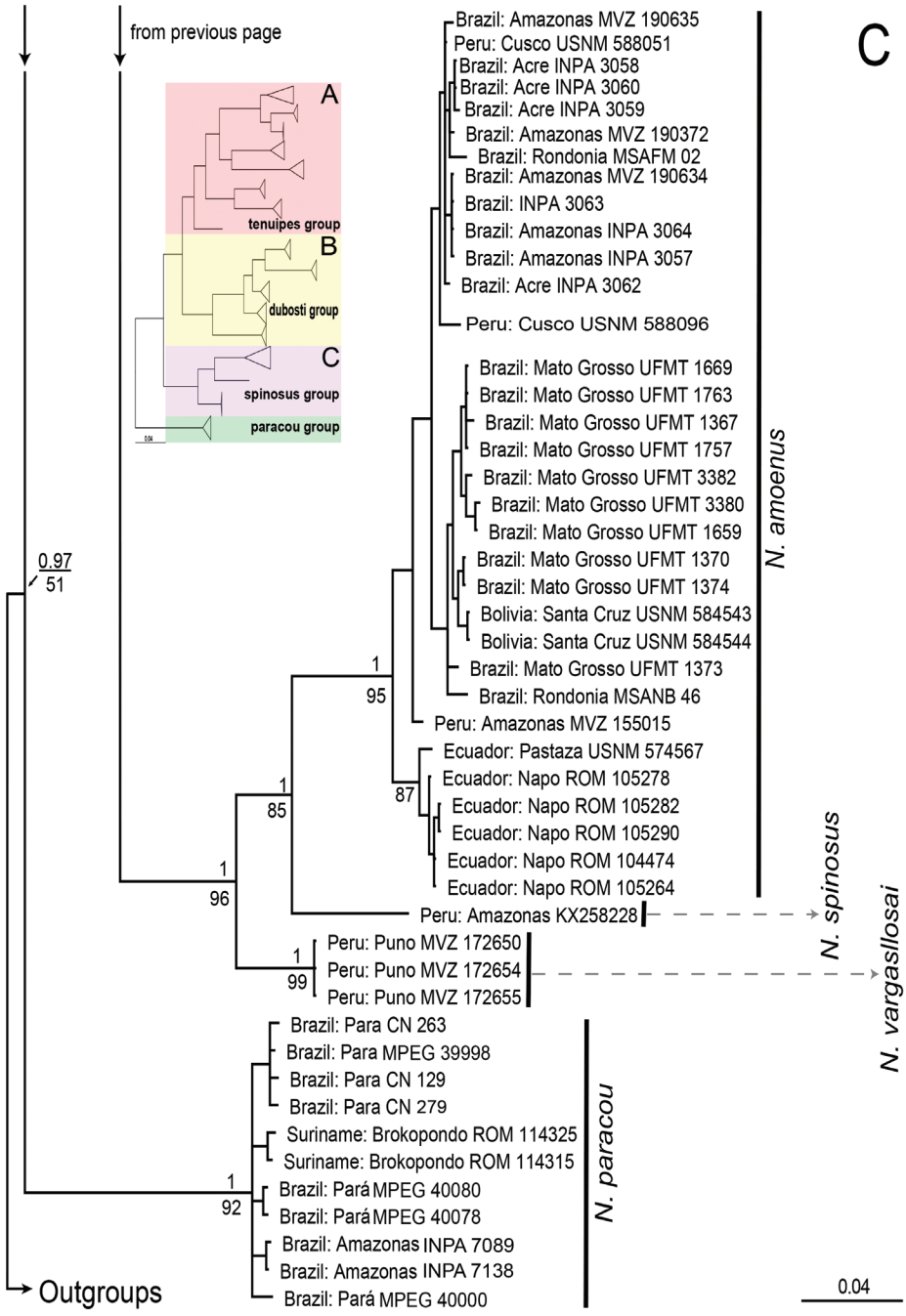
from previous page
A
tenuipes group
B
dubosti group
C
spinosus group
paracou group
0.04
C
Brazil: Amazonas MVZ 190635
Peru: Cusco USNM 588051
Brazil: Acre INPA 3058
Brazil: Acre INPA 3060
Brazil: Acre INPA 3059
Brazil: Amazonas MVZ 190372
Brazil: Rondonia MSAFM 02
Brazil: Amazonas MVZ 190634
Brazil: INPA 3063
Brazil: Amazonas INPA 3064
Brazil: Amazonas INPA 3057
Brazil: Acre INPA 3062
Peru: Cusco USNM 588096
Brazil: Mato Grosso UFMT 1669
Brazil: Mato Grosso UFMT 1763
Brazil: Mato Grosso UFMT 1367
Brazil: Mato Grosso UFMT 1757
Brazil: Mato Grosso UFMT 3382
Brazil: Mato Grosso UFMT 3380
Brazil: Mato Grosso UFMT 1659
Brazil: Mato Grosso UFMT 1370
Brazil: Mato Grosso UFMT 1374
Bolivia: Santa Cruz USNM 584543
Bolivia: Santa Cruz USNM 584544
Brazil: Mato Grosso UFMT 1373
Brazil: Rondonia MSANB 46
Peru: Amazonas MVZ 155015
Ecuador: Pastaza USNM 574567
Ecuador: Napo ROM 105278
Ecuador: Napo ROM 105282
Ecuador: Napo ROM 105290
Ecuador: Napo ROM 104474
Ecuador: Napo ROM 105264
Peru: Amazonas KX258228
Peru: Puno MVZ 172650
Peru: Puno MVZ 172654
Peru: Puno MVZ 172655
Brazil: Para CN 263
Brazil: Para MPEG 39998
Brazil: Para CN 129
Brazil: Para CN 279
Suriname: Brokopondo ROM 114325
Suriname: Brokopondo ROM 114315
Brazil: Pará MPEG 40080
Brazil: Pará MPEG 40078
Brazil: Amazonas INPA 7089
Brazil: Amazonas INPA 7138
Brazil: Pará MPEG 40000
Outgroups
N. amoenus
N. spinosus
N. vargasllosai
N. paracou
0.97
51
1
95
1
85
87
1
96
1
99
1
92

TABLE 3. Descriptive statistics for external and craniodental dimensions (in mm) and mass (in g) of species in the Dubosti Group of *Neacomys*.

	dubosti	*marajoara*	*xingu*	*vossi*
TL	157 ± 7 148–167 (9)	144 ± 10 128–153 (9)	146 ± 5 138–156 (7)	140 ± 13 110–156 (14)
HBL	79 ± 4 74–88 (9)	72 ± 4 62–77 (9)	71 ± 2 68–75 (7)	68 ± 10 65–77 (14)
LT	77 ± 4 71–83 (9)	72 ± 8 55–79 (9)	74 ± 5 68–85 (7)	72 ± 6 60–84 (14)
HF	21 ± 1 20–23 (9)	17 ± 2 13–19 (9)	20 ± 3 14–26 (7)	16 ± 3 10–20 (14)
Ear	14 ± 1 12–15 (9)	12 ± 1 11–14 (9)	12 ± 1 11.5–14.5 (6)	12 ± 3 8–19 (14)
Mass	15 ± 3 12–20 (9)	12 ± 2 9–16.5 (9)	14 ± 3 11.5–18.5 (7)	12 ± 2 9–15.5 (14)
BH	7.14 ± 0.27 6.61–7.48 (12)	6.7 ± 0.32 6.33–7.08 (7)	6.77 ± 0.2 6.4–7 (13)	6.71 ± 0.38 6.02–7.24 (8)
BIF	1.51 ± 0.1 1.39–1.68 (12)	1.40 ± 0.08 1.30–1.55 (7)	1.41 ± 0.11 1.21–1.58 (13)	1.44 ± 0.09 1.31–1.56 (8)
BM1	0.90 ± 0.04 0.82–0.98 (12)	0.85 ± 0.03 0.81–0.88 (7)	0.87 ± 0.04 0.80–1.01 (13)	0.85 ± 0.08 0.75–0.97 (8)
BPR	4.02 ± 0.18 3.73–4.32 (12)	3.76 ± 0.27 3.37–4.06 (7)	4.09 ± 0.20 3.70–4.47 (13)	3.92 ± 0.27 3.50–4.34 (8)
BZP	2.06 ± 0.19 1.86–2.58 (12)	1.84 ± 0.11 1.67–1.97 (7)	1.99 ± 0.23 1.73–2.62 (13)	1.88 ± 0.07 1.80–2.01 (8)
BB	3.66 ± 0.18 3.38–3.93 (12)	3.46 ± 0.22 3.17–3.8 (7)	3.63 ± 0.17 3.39–3.92 (13)	3.51 ± 0.11 3.43–3.75 (8)
CIL	18.57 ± 0.59 17.38–19.43 (12)	17.51 ± 0.36 16.92–18.06 (7)	18.06 ± 0.58 17.44–19.28 (13)	17.37 ± 0.48 16.75–18.3 (8)
LCIB	8.13 ± 0.97 5.33–8.96 (12)	7.71 ± 0.3 7.13–7.97 (7)	8.17 ± 0.53 7.34–9.36 (13)	7.93 ± 0.27 7.58–8.34 (8)
LIB	4.65 ± 0.12 4.47–4.87 (12)	4.47 ± 0.2 4.23–4.74 (7)	4.56 ± 0.26 4.11–4.93 (13)	4.46 ± 0.18 4.25–4.77 (8)
LD	5.36 ± 0.25 4.94–5.69 (12)	5.01 ± 0.20 4.69–5.28 (7)	5.06 ± 0.15 4.74–5.37 (13)	4.92 ± 0.14 4.80–5.20 (8)
LIF	2.98 ± 0.26 2.64–3.47 (12)	2.99 ± 0.10 2.83–3.16 (7)	2.98 ± 0.23 2.48–3.26 (13)	2.91 ± 0.30 2.53–3.57 (8)
LLD	3.0 ± 0.30 2.24–3.3 (12)	2.89 ± 0.23 2.47–3.14 (7)	2.87 ± 0.18 2.43–3.08 (13)	3.34 ± 0.99 2.64–4.96 (8)
LLM	2.97 ± 0.13 2.56–3.06 (12)	2.77 ± 0.04 2.71–2.82 (7)	2.92 ± 0.08 2.8–3.13 (13)	2.77 ± 0.08 2.64–2.87 (8)
LM	2.75 ± 0.07 2.63–2.84 (12)	2.53 ± 0.06 2.42–2.61 (7)	2.75 ± 0.09 2.60–2.90 (13)	2.58 ± 0.08 2.45–2.65 (8)
LN	7.81 ± 0.35 7.23–8.51 (12)	7.45 ± 0.45 6.62–7.90 (7)	7.89 ± 0.46 7.02–8.90 (13)	7.24 ± 0.39 6.56–7.84 (8)

	dubosti	*marajoara*	*xingu*	*vossi*
LPB	3.95 ± 0.27 3.49–4.45 (12)	3.65 ± 0.18 3.31–3.85 (7)	3.87 ± 0.24 3.40–4.25 (13)	3.66 ± 0.18 3.46–4.06 (8)
MB	8.86 ± 0.23 8.53–9.27 (12)	8.27 ± 0.22 8.02–8.64 (7)	8.51 ± 0.22 8.27–8.92 (13)	8.34 ± 0.12 8.20–8.50 (8)
OL	7.19 ± 0.33 6.45–7.76 (12)	6.94 ± 0.16 6.74–7.12 (7)	7.04 ± 0.28 6.51–7.44 (13)	6.7 ± 0.33 6.16–7.28 (8)
RB	3.77 ± 0.24 3.41–4.40 (12)	3.80 ± 0.20 3.43–4.06 (7)	3.89 ± 0.30 3.3–4.43 (13)	3.77 ± 0.16 3.48–3.95 (8)
RL	6.58 ± 0.26 6.12–6.98 (12)	6.36 ± 0.32 5.84–6.68 (7)	6.58 ± 0.33 6.09–7.20 (13)	6.06 ± 0.48 5.43–6.82 (8)
ZB	11.15 ± 0.43 10.46–11.78 (12)	10.51 ± 0.20 10.21–10.76 (7)	10.91 ± 0.41 9.93–11.51 (13)	10.52 ± 0.30 10.13–11.05 (8)

TAXONOMIC ACCOUNTS

Our molecular analyses revealed the existence of 17 lineages of *Neacomys* with high levels of genetic divergence; of these, four occur in southeastern Amazonia (south of the Amazon River and east of the Rio Madeira). Although not strongly morphometrically differentiated, these previously unnamed southeastern lineages can be recognized as species based on our molecular analyses (which provide evidence of mtDNA divergence), by the karyotypic traits previously reported in the literature (which suggest they are reproductively isolated), and by qualitative morphological characters (which provide evidence of nuclear-gene divergence). Three of these species are described below, whereas the fourth (*Neacomys* "sp. 2") will be described in another report with different authorship. Because all the new species belong to the Dubosti Group, our comparisons are restricted to members of that clade. Relevant summaries of morphometric variation and diagnostic traits are provided in tables 3 and 4, respectively.

Neacomys marajoara, new species

Marajoara Spiny Mouse
Figures 4, 7

Holotype: The holotype (MPEG 40432) is an adult male (age class 3), collected on 19 January 2009, by R.V. Rossi (field number MAJ 23; fig. 4) in a pitfall trap. The specimen consists of a stuffed skin (missing the tip of the tail), skull, and skeleton; a tissue sample of this specimen is preserved in ethanol, and a partial cytochrome *b* sequence that we obtained from it has been deposited in Genbank with accession number MT462070.

Type Locality: Tauari Farm, municipality of Chaves, Marajó Island, state of Pará, Brazil (0°39′S, 50°11′W, figs. 5, 6).

Diagnosis: *Neacomys marajoara* is a small species (table 3) that differs from congeneric taxa by the following combination of craniodental traits: skull delicate; interorbital region rela-

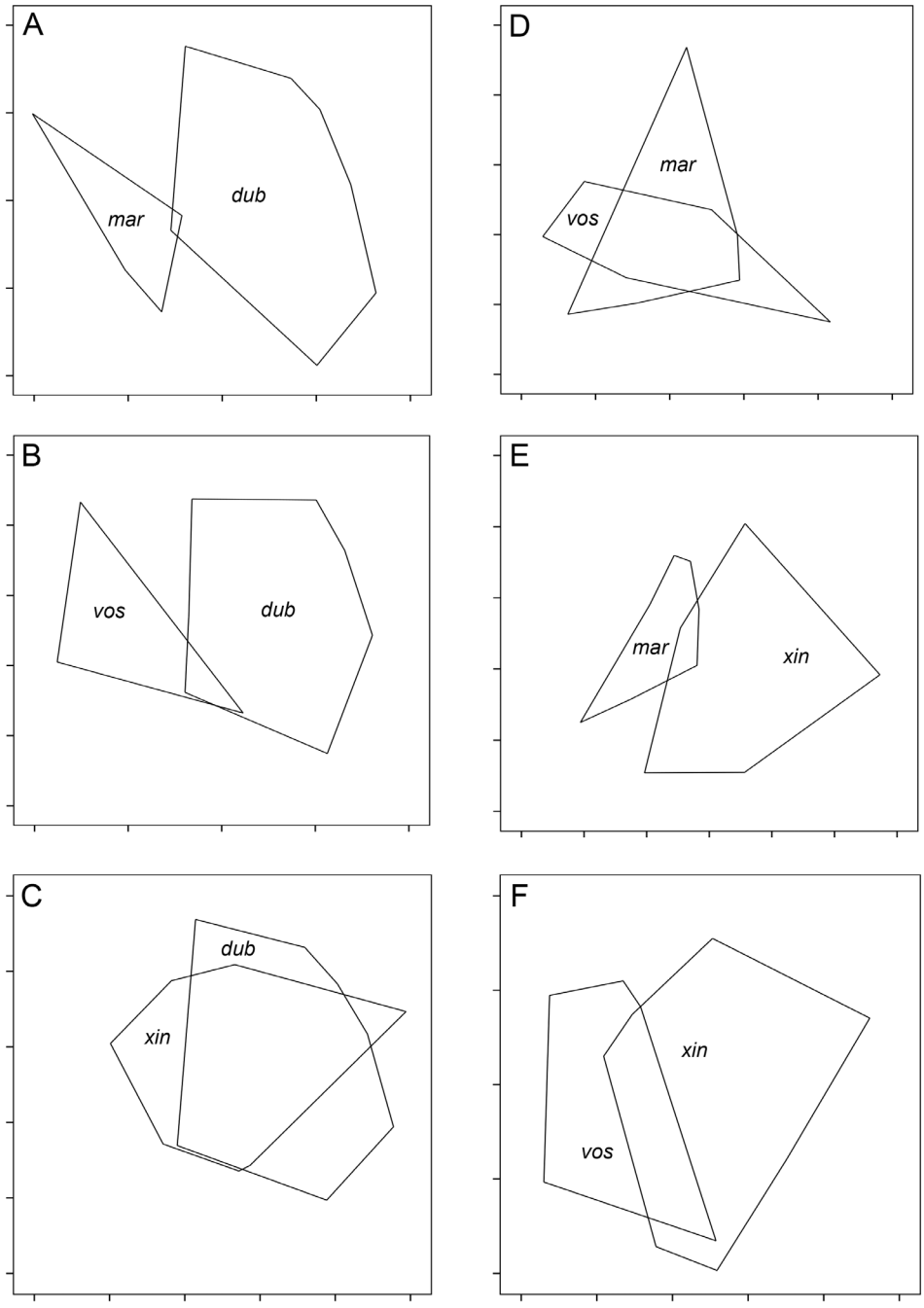

FIG. 3. Scatter plots of PC1 (horizontal axis) and PC2 (vertical axis) for pairwise analyses of craniodental measurement data for species in the Dubosti Group of *Neacomys*. In each plot, species are represented by minimum convex polygons that enclose all points in the plane of PC1 and PC2. **A,** *N. dubosti* (dub) versus *N. marajoara* (mar); **B,** *N. dubosti* versus *N. vossi* (vos); **C,** *N. dubosti* versus *N. xingu* (xin); **D,** *N. marajoara* versus *N. vossi*; **E,** *N. marajoara* versus *N. xingu*; **F,** *N. vossi* versus *N. xingu.*

FIG. 4. The holotype of *Neacomys marajoara*, (MPEG 40432) in life. Photo by Rogério V. Rossi.

tively broad; nasal bones straight anteriorly; supraorbital margins slightly convergent anteriorly; subsquamosal fenestra large (almost half the size of the postglenoid foramen on each side of the skull); paraoccipital processes separated from the auditory bullae; sphenopalatine foramen large; carotid circulation usually pattern 2 (sensu Voss, 1988); maxillary part of incisive septum (between the incisive foramina) narrow; M1 usually with flat and undivided anterocone; and M1 anteroloph usually fused with anterolabial conule.

Morphological Description: Dorsal pelage dark brown finely sprinkled with orange (fig. 4); ventral pelage varying from pure white to yellowish white, separated from the dorsal pelage by a very thin orange lateral line. Superciliary, genal, and mystacial vibrissae blackish and long (extending behind ears when laid back alongside the head); submental vibrissae absent; interramal vibrissae short and white. Ears small and rounded; postauricular hairs gray based with orange tips, forming an orange tuft behind each pinna. Ungual tufts white, longer than claws in most specimens examined (except MPEG 40435 and MPEG 40446, in which ungual tufts are as long as the claws); fore- and hind feet covered dorsally with buffy-cream hairs; hind feet narrow and elongate with small interdigital membranes present. Tail about the same length as head and body, bicolored, and covered by short, spiny, and clearly visible hairs; white hairs present on ventral caudal surface from base to midlength; tail tip with very short

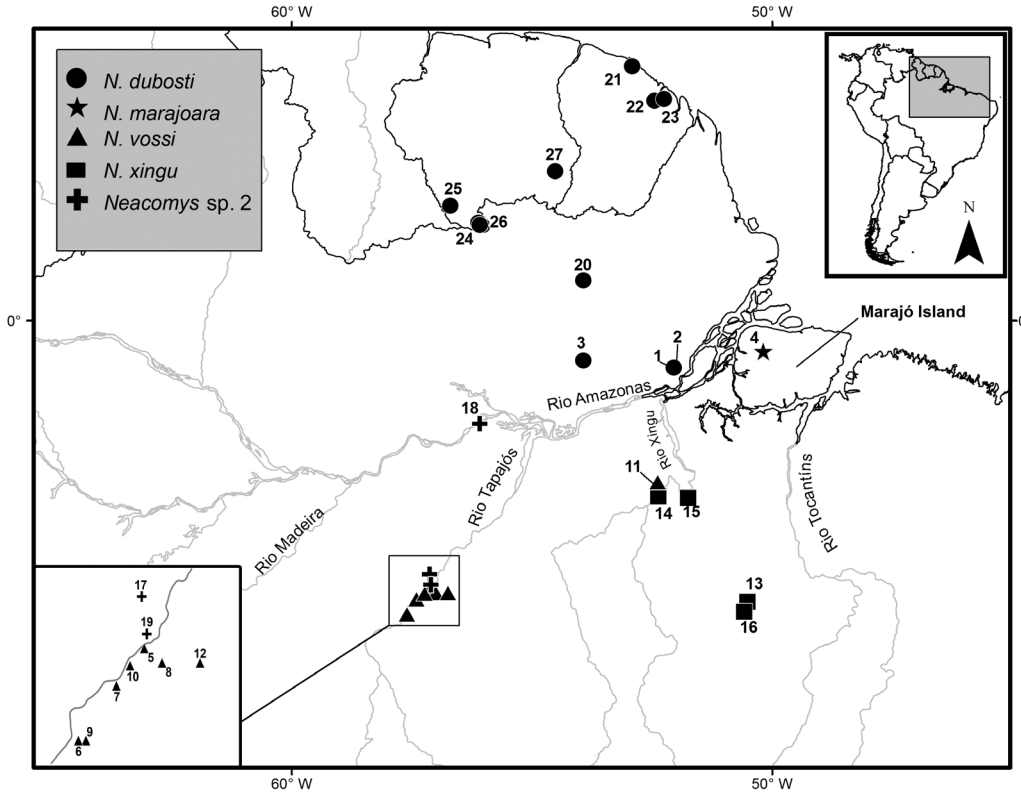

FIG. 5. Collection localities of specimens of the Dubosti Group of *Neacomys* examined in the present study. Numbers are keyed to entries in our gazetteer (appendix 1).

(1 mm) terminal tuft; caudal scales small, arranged in annular series; each caudal scale with three subequal hairs inserted along its posterior margin.

Skull small and delicate in dorsal view (fig. 7), with straight anterior nasal margins, notably broad rostrum, and shallow zygomatic notches; posterior nasal terminus usually slightly pointed, extending beyond maxillary-frontal suture; premaxillaries terminating anterior to nasals; lacrimal bone small and visible in dorsal view, usually in broad contact with frontal bones; supraorbital margins slightly convergent anteriorly; interorbital region relatively broad; supraorbital beads developed as projecting shelves; lateral expansion of the parietal restricted to the dorsal cranial surface. Incisive foramina small and usually teardrop shaped, not extending posteriorly to level of M1s; maxillary portion of incisive septum (dividing the left and right foramina) narrow. Zygomatic plate narrow. Palate with two posterolateral pits on each side. Auditory bullae small and globular, with short and narrow eustachian tubes; periotic bone extends anteriorly to internal carotid canal (except MPEG 40435, MPEG 40443, and MPEG 40439, in which the periotic does not reach the internal carotid canal), but does not enter the canal. Subsquamosal fenestra large (almost half the size of the postglenoid foramen); hamular process of the squamosal long. Paraoccipital process narrow and small and separated from the auditory bullae. Sphenopalatine foramen large; alisphenoid strut absent; carotid circulation

FIG. 6. Habitat of *Neacomys marajoara* at Tauari Farm, municipality of Chaves, Marajó Island, state of Pará, Brazil. Photo by Rogério V. Rossi.

pattern usually derived[7] (pattern 2, as identified by the presence of a large stapedial foramen and a large posterior opening of the alisphenoid canal, and by the absence of a squamosal-alisphenoid groove and a sphenofrontal foramen; Voss, 1988).

First upper molar (M1) usually with broad, flat, and undivided anterocone; anteroloph usually fused with anterolabial conule (such that the anteroflexus is not distinguishable); M3 small; labial cusps (paracone and metacone) usually smaller than lingual cusps (protocone and hypocone); m1 anterocone undivided.

Mandible with mental foramen opening laterally; capsular process of lower incisor alveolus present, but indistinct (reduced to a slight rounded elevation), approximately at same height as coronoid process.

Karyotypes: Karyotypes of specimens from the type locality were obtained by Silva et al. (2015), and karyotypes from specimens collected elsewhere on Marajó Island were obtained

[7] Most specimens of *Neacomys marajoara* (seven out of nine) exhibit carotid circulation pattern 2, but one specimen (MPEG 40446) exhibits circulatory pattern 1, and another (MPEG 40431) exhibits both patterns (on opposite sides of the skull).

FIG. 7. Dorsal, ventral, and lateral cranial views and lateral view of mandible of *Neacomys marajoara* (MPEG 40432, holotype).

by Oliveira da Silva et al. (2019), who described a chromosomal complement of $2n = 58$ and a fundamental number (FN) = 70 (table 5).

Taxonomic Comparisons: *Neacomys marajoara* differs from *N. dubosti* in dorsal pelage color (dark brown finely sprinkled with orange versus light to dark brown finely sprinkled with orange in *N. dubosti*), and by its bicolored tail (the tail is usually unicolored in *N. dubosti*), narrower interorbital region, teardrop-shaped incisive foramina (the lateral margins of the incisive foramina are usually subparallel in *N. dubosti*), globular auditory bullae (the bullae are usually flask-shaped in *N. dubosti*), and carotid circulation usually pattern 2 (versus pattern 1 in *N. dubosti*).

TABLE 4. Geographic and morphological comparisons among members of the Dubosti Group of *Neacomys*.

	dubosti	*xingu*	*marajoara*	*vossi*
Distribution	NE Amazonia	SE Amazonia	SE Amazonia	SE Amazonia
Dorsal pelage	light to dark brown finely sprinkled with orange	orange-brown sprinkled with black	dark brown finely sprinkled with orange	brown sprinkled with orange and/or black
Ventral pelage	pure white to buffy white	pure white to buffy white	pure white to yellowish white	pure white to buffy white
Tail	usually unicolored	usually unicolored	bicolored	usually slightly bicolored
Nasal bones	–	expanded anteriorly	straight anteriorly	expanded anteriorly
Interorbital region	broad	narrow	relatively broad	narrow
Paraoccipital process	–	usually separated from auditory bullae	separated from auditory bullae	close to the auditory bullae
Subsquamosal fenestrae	–	small	large	usually small
Sphenopalatine foramen	–	small	large	large
Lateral expansion of parietal	restricted	slightly expanded to restricted	restricted	slightly expanded to restricted
Carotid circulation	pattern 1	usually pattern 1[a]	usually pattern 2[b]	pattern 1
Incisive foramina	small and usually subparallel	small and subparallel	small and usually teardrop shaped	small and subparallel
Maxillary septum of incisive foramina	–	wide	narrow	usually wide
Zygomatic plate	narrow	narrow to broad	narrow	narrow
Auditory bullae	usually flask-shaped	usually globular	globular	globular
M1 anteroloph	–	fused	fused or distinct	usually distinct

[a] We found variation in this character, please see *Neacomys xingu* description.
[b] We found variation in this character, please see *Neacomys marajoara* description.

Neacomys marajoara differs from *N. xingu* in dorsal pelage color (dark brown finely sprinkled with orange versus orange-brown sprinkled with black in *N. xingu*), and by its bicolored tail (the tail is usually unicolored in *N. xingu*), anteriorly straight (versus anteriorly expanded) nasal bones, broader interorbital region, narrower maxillary septum of the incisive foramina, larger subsquamosal fenestrae, and carotid circulation usually pattern 2 (versus usually pattern 1).

Neacomys marajoara differs from *N. vossi* in dorsal pelage color (dark brown finely sprinkled with orange versus brown sprinkled with orange and/or black in *N. vossi*), and by its anteriorly straight (versus anteriorly expanded) nasal bones, broader interorbital region, paraoccipital processes separated from the auditory bullae (versus processes close to the auditory bullae), larger subsquamosal fenestrae, carotid circulation usually pattern 2 (versus pattern 1), and narrower maxillary septum of the incisive foramina.

Karyotypically, *Neacomys marajoara* differs from other species in the Dubosti Group by having a diploid chromosomal complement of 58 (versus $2n = 64$ in *N. dubosti*; table 5), a uniquely large FN of 70 autosomal arms (versus FN = 64–68 in other group members), and submetacentric sex chromosomes (at least one of the sex chromosomes is acrocentric in *N. dubosti* and "species 2").

Distribution: *Neacomys marajoara* has been recorded only on Marajó Island, state of Pará, Brazil (fig. 5).

Etymology: The specific epithet *marajoara* is to be treated as a noun in apposition. It is derived from Tupi Guarani (a language family that comprises many different indigenous Amazonian dialects) and denotes a native of Marajó Island (the type locality).

Field Notes: Of the nine specimens for which trapping information is available, eight were captured in pitfall traps and one was taken in a Sherman trap placed on the ground. One paratype (MPEG 40435) was pregnant with three fetuses.

Remarks: *Neacomys marajoara* was previously reported in the literature as "*Neacomys* sp." (in part) by Silva at al. (2015) and as "*Neacomys* sp. D" by Oliveira da Silva et al. (2019).

Neacomys vossi, new species

Voss's Spiny Mouse
Figures 8, 9

Holotype: The holotype (UFPA 1583) is an adult female (age class 2) collected on 2 April 2013, by Ana Cristina Mendes Oliveira (original field number JB 031). The specimen consists of a stuffed skin, skull, and skeleton, all in good condition; additionally, a tissue sample is preserved in ethanol, and a partial cytochrome *b* sequence that we obtained from it has been deposited in Genbank with accession number MT462028.

Type Locality: Boca do Rato, on the right bank of the Rio Tapajós, Itaituba municipality, state of Pará, Brazil (5°14′S, 56°56′W, fig. 5).

Diagnosis: *Neacomys vossi* is a small species (table 3) that differs from congeneric taxa by the following combination of craniodental traits: skull delicate; interorbital region narrow; nasal bones expanded anteriorly; supraorbital margins convergent anteriorly; subsquamosal fenestra usually small (about ¼ the size of the postglenoid foramen on each side of the skull); paroccipital processes close to the auditory bullae; sphenopalatine foramen large; carotid circulation pattern 1 (sensu Voss, 1988); maxillary part of incisive septum (between the incisive foramina) usually wide; M1 usually with slightly flat, narrow, and undivided anterocone; and M1 anteroloph usually distinct (not fused with the anterolabial conule).

Morphological Description: Dorsal pelage brown sprinkled with orange and/or black (fig. 8); ventral pelage varying from pure white to buffy white; very thin orange lateral line. Superciliary, genal, and mystacial vibrissae blackish and long (extending behind ears when laid back alongside the head); submental vibrissae absent; interramal vibrissae short and white. Ears small and rounded; post-auricular hairs gray-based with orange tips, forming an orange tuft behind each pinna. Ungual tufts white, longer than claws; fore- and hind feet covered dorsally with buffy-cream hairs; hind feet narrow and elongate with small interdigital membranes. Tail about the same length as head and body, usually slightly bicolored (except in UFPA 1277, 1417, 1444, 1654, and 1736 which have unicolored tail) and covered by spiny and clearly visible hairs; tail tip of the tail with very short (approximately 1.4 mm long) terminal tuft; caudal scales small, arranged in annular series; each caudal scale with three subequal hairs inserted along its posterior margin.

Skull small and delicate in dorsal view (fig. 9); with expanded anterior nasal margins; notably broad rostrum and shallow zygomatic notches; posterior nasal terminus usually flat, extending beyond the maxillary-frontal suture; premaxillaries terminating slightly anterior to nasals; lacrimal bone small and visible in dorsal view, equally contacting maxillary and frontal bones; supraorbital margins convergent anteriorly; interorbital region narrow; supraorbital beads developed as projecting shelves; lateral expansion of the parietal restricted to the dorsal surface (except in UFPA 1227 and UFPA 1577, in which the parietal is slightly expanded ventrally near the squamosal root of the zygomatic arch). Incisive foramina small with subparallel lateral margins, not extending posteriorly to the level of M1s; maxillary portion of incisive septum (dividing the left and right foramina) usually wide. Zygomatic plate narrow. Palate with two posterolateral pits on each side of the palate. Auditory bullae small and globular, with short and narrow eustachian tubes; periotic bone extending anteriorly to internal carotid canal, but usually not entering into it (except in UFPA 1227, 1417, 1530, 1654, 1417, and 1736, in which the periotic does enter the internal carotid canal). Subsquamosal fenestra usually small (about ¼ the size of the postglenoid foramen); hamular process of the squamosal long. Paraoccipital process narrow, small, and close to the auditory bullae (Sánchez-Vendizú et al., 2018: fig. 3C). Sphenopalatine foramen large; alisphenoid strut absent; carotid circulation primitive (pattern 1, as identified by retaining a well-developed squamosal-alisphenoid groove and sphenofrontal foramen, both indicative of the presence of the supraorbital branch of the stapedial artery; Voss et al., 1988).

First upper molar (M1) usually with slightly flat and undivided anterocone; anteroloph usually distinct (not fused with the anterolabial conule); M3 small; labial cusps (paracone, metacone) usually taller than lingual cusps (protocone, hypocone); m1 anteroconid undivided.

Mandible with mental foramen opening laterally; capsular process of lower incisor alveolus present, but indistinct (reduced as a slight, rounded elevation), approximately at same height as coronoid process.

Taxonomic Comparisons: *Neacomys vossi* differs from *N. dubosti* in dorsal pelage color (brown sprinkled with orange and/or black versus dark brown finely sprinkled with orange in

FIG. 8. Dorsal and ventral views of the skin of *Neacomys vossi* (UFPA 1583, holotype).

FIG. 9. Dorsal, ventral, lateral cranial views and lateral view of mandible of *Neacomys vossi* (UFPA 1583, holotype).

FIG. 10. Robert S. Voss in the field (Venezuela, 1979; photo by Paul Kaarakka).

N. dubosti), and by its narrower interorbital region, and globular auditory bullae (the bullae are usually flask shaped in *N. dubosti*).

Neacomys vossi differs from *N. xingu* in dorsal pelage color (brown sprinkled with orange and/or black versus orange-brown sprinkled with black in *N. xingu*), larger sphenopalatine foramen, and an M1 anteroloph that is usually distinct (versus fused in *N. xingu*).

Karyotypically, *Neacomys vossi* differs from other species in the Dubosti Group by having a diploid chromosome complement of 58 (versus $2n = 64$ in *N. dubosti* and $2n = 64$ in "species 2"), an FN of 68 autosomal arms (versus FN = 70 in *N. marajoara*, FN = 64 in *N. xingu*, and FN = 66 in "species 2"), and submetacentric sex chromosomes (at least one of the sex chromosomes is acrocentric in *N. dubosti* and "species 2").

Distribution: *Neacomys vossi* has been collected on the right bank of the upper and middle Tapajós River and on the left bank of lower Xingu (fig. 5). According to our records, the species appears to be endemic to the Tapajós center of endemism (Silva et al., 2005).

Etymology: Named in honor of Robert S. Voss (fig. 10), curator of mammals at the American Museum of Natural History, New York, for his extensive contributions to our knowledge of Neotropical mammals, especially the taxonomy of *Neacomys* in northeastern Amazonia.

Field Notes: Among the specimens we examined for which trapping information is available, all 17 were captured in pitfall traps, two (UFPA 1277 and 1284) in upland (*terra firme*) forests and three (UFPA 1444, 1487, and 1583) in primary forest of unknown character.

Remarks: *Neacomys vossi* was previously reported in the literature as "*Neacomys* sp. A" by Oliveira da Silva et al. (2017, 2019).

***Neacomys xingu*, new species**

Xingu Spiny Mouse
Figures 11, 12

Holotype: The holotype (UFMT 1268) is an adult female (age class 5), collected on 28 August 2009 by Cleuton Lima Miranda (original field number PSA 242) in a pitfall trap. The specimen is preserved as a skin, skull, and skeleton in good condition; additionally, a tissue is

preserved in alcohol, and a partial cytochrome *b* sequence that we obtained from it has been deposited in Genbank with accession number MT462060.

Type Locality: Flona Tapirapé-Aquiri, Marabá, state of Pará, Brazil (5°46′S, 50°32′W, fig. 5).

Diagnosis: *Neacomys xingu* is a small species (table 3) that differs from congeneric taxa by the following combination of craniodental traits: skull delicate; interorbital region narrow; nasal bones expanded anteriorly; supraorbital margins convergent anteriorly; subsquamosal fenestra small (about ¼ the size of the postglenoid foramen on each side of the skull); paraoccipital process separated from the auditory bullae; sphenopalatine foramen small; carotid circulation usually pattern 1 (sensu Voss, 1988); maxillary part of incisive septum (between the incisive foramina) wide; M1 usually with flat and undivided anterocone; and M1 anteroloph fused with the anterolabial conule.

Morphological Description: Dorsal pelage orange-brown, sprinkled with black (fig. 11); ventral pelage varying from pure white to buffy white and separated from the dorsal pelage by a thin orange lateral line. Superciliary, genal, and mystacial vibrissae blackish and long (extending behind ears when laid back alongside the head); submental vibrissae absent; interramal vibrissae short and white; Ears small and rounded; postauricular hairs gray based with orange tips, forming an orange tuft behind each pinna. Ungual tufts white, longer than claws in length; fore- and hind feet covered dorsally with buffy-cream hairs; hind feet narrow and elongate with small interdigital membranes present. Tail about the same length as head and body, usually unicolored (except in PSA 069, MPEG 39901, and MPEG 42019, in which the tail is dark above and paler below), and covered by short, spiny, and clearly visible hairs; tail tip with very short (1–2 mm) terminal tuft; caudal scales small, arranged in annular series; each caudal scale with three subequal hairs inserted along its posterior margin.

Skull small and delicate in dorsal view (fig. 12); with anteriorly expanded nasal margins; notably broad rostrum and shallow zygomatic notches; posterior nasal terminus slightly pointed, extending beyond the maxillary-frontal suture; premaxillaries terminating slightly anterior to nasals; lacrimal bone small and visible in dorsal view, equally contacting the maxillary and frontal bones; supraorbital margins convergent anteriorly; interorbital region narrow; supraorbital beads developed as projecting shelves; lateral expansion of the parietal restricted to the dorsal cranial surface (except in MCN-M 1404 and MPEG 39901, in which the parietal is slightly expanded ventrally near the squamosal root of the zygomatic arch). Incisive foramina small with subparallel lateral margins, not extending posteriorly to level of M1s; maxillary portion of incisive septum (dividing the left and right foramina) usually wide. Zygomatic plate varying from broad to narrow. Palate with two posterolateral pits on each side. Auditory bullae small and usually globular, with short and narrow eustachian tubes; periotic bone extends anteriorly to the internal carotid canal but does not enter it (except in MPEG 42715 and MCN-M 1404, in which the periotic does not reach the internal carotid canal). Subsquamosal fenestra small (about ¼ the size of the postglenoid foramen); hamular process of the squamosal long. Paraoccipital process narrow and small and usually separated from the auditory bullae (Sánchez-Vendizú et al., 2018: fig. 3C). Sphenopalatine foramen small (except in MPEG 41991,

FIG. 11. Dorsal and ventral views of the skin of *Neacomys xingu* (UFMT 1268, holotype).

whose sphenopalatine foramen is large); alisphenoid strut absent; carotid circulation pattern usually primitive[8] (pattern 1, as identified by retaining a well-developed squamosal-alisphenoid groove and sphenofrontal foramen, both indicative of the presence of the supraorbital branch of the stapedial artery; Voss, 1988: fig. 18A, B).

First upper molar (M1) usually with slightly flat and undivided anterocone; anteroloph usually fused with the anterolabial conule (such that the anteroflexus is not distinguishable); M3 small; labial cusps (paracone, metacone) usually taller than lingual cusps (protocone, hypocone); m1 anteroconid undivided.

Mandible with mental foramen opening laterally; capsular process of lower incisor alveolus present, but indistinct (reduced to a slight rounded elevation), approximately at same height of coronoid process.

Taxonomic Comparisons: *Neacomys xingu* differs from *N. dubosti* in dorsal pelage color (orange-brown sprinkled with black versus light to dark brown finely sprinkled with orange), and by its narrower interorbital region, globular auditory bullae (the bullae are usually flask shaped in *N. dubosti*), and carotid circulation usually pattern 1 (versus always pattern 1 in *N. dubosti*).

Karyotypically, *Neacomys xingu* differs from all other members of the Dubosti Group by having a diploid chromosomal complement of 58 (versus $2n = 64$ in *N. dubosti* and $2n = 54$ in "species 2"), a uniquely small FN of 64 autosomal arms (versus FN = 66–60 in other species), and submetacentric sex chromosomes (at least one sex chromosome is acrocentric in *N. dubosti* and "species 2").

Distribution: *Neacomys xingu* has been collected on the right bank of the lower Xingu River and in the region of Serra de Carajás, in southeastern Pará state (fig. 5). According to cytogenetic data (Di-Nizo et al., 2017; Oliveira da Silva et al., 2019), the species also ranges southward into Vila Rica in northeastern Mato Grosso state. These records suggest that the species is restricted to the Xingu center of endemism (Silva et al., 2005).

Etymology: The specific epithet *xingu* is to be treated as a noun in apposition. The species name refers to the Xingu center of endemism, delimited by the Xingu and Tapajós rivers, where the species occurs.

Remarks: *Neacomys xingu* was previously reported in the literature as "*Neacomys* clade 7" by Patton et al. (2000), "*Neacomys* sp." (in part) by Silva at al. (2015), "*Neacomys* sp." by Di-Nizo et al. (2017) and Brandão et al. (2019), and "*Neacomys* sp. C" by Oliveira da Silva et al. (2019).

DISCUSSION

This study includes the largest mitochondrial DNA dataset yet assembled for *Neacomys*, the results of which support generic monophyly, as have all previous analyses of *Cytb* sequence data (Catzflies and Tilak, 2009; Silva et al., 2015; Hurtado and Pacheco, 2017; Sánchez-Vendizú et al., 2018). Our analyses additionally reveal the existence of 17 distinct

[8] Most specimens of *Neacomys xingu* have carotid circulation pattern 1, whereas four specimens had circulatory pattern 2 (MPEG 40446, MPEG 39901, MCN-M 1403, and MCN-M 1404).

FIG. 12. Dorsal, ventral, lateral cranial views and lateral view of mandible of *Neacomys xingu* (UFMT 1268, holotype).

lineages clustered in four main groups. Two of these groups correspond to the Paracou and Spinosus groups of Hurtado and Pacheco (2017) and Sánchez-Vendizú et al. (2018), but the inclusion of new sequence data from southeastern Amazonia in our analyses make it expedient to restrict the membership of their Tenuipes Group and to recognize a fourth clade, which we refer to as the Dubosti Group.

The three new species herein described—*N. marajoara*, *N. xingu*, and *N. vossi*—belong to the Dubosti Group. These species, together with an unnamed member species ("species 2"), have genetic divergences varying from 3.9% to 9.4%, comparable to distances previously reported for recently described species such as *N. vargasllosai* and *N. spinosus* (7.8%; Hurtado

TABLE 5. Karyotypes [a] of *Neacomys* species in the Dubosti Group.

	2*n*	FN	gA	gB	gC	gD	X	Y	Source
dubosti	64	68	—	6	—	56	SM	A	Silva et al., 2015
marajoara	58	70	—	14/8	—	42/48	SM	SM	Silva et al., 2015
vossi	58	68	—	12	—	44	SM	SM	Oliveira da Silva et al., 2017
xingu	58	64	—	8	—	48	SM	SM	Silva et al., 2015
species 2	54	66	8	6	—	38	A	A	Oliveira da Silva et al., 2017

[a] Diploid number (2*n*); fundamental number (FN); group A (gA) = large metacentric and submetacentric autosomes; group B (gB) = medium and small metacentric or submetacentric autosomes; group C (gC) = medium and small subtelocentric autosomes; group D (gD) = large, medium, and small acrocentric autosomes. Abbreviations for sex chromosome (X and Y) morphology: M = metacentric, SM = submetacentric, ST = subtelocentric, A = acrocentric.

and Pacheco, 2017), and *N. macedoruizi* and the "upriver" clade of *N. minutus* (4.9%; Sánchez-Vendizú et al., 2018). Although *N. marajoara* and *N. xingu* have the lowest genetic divergence value (3.9%) reported for any pair of *Neacomys* species, this value is within the known range of interspecific mammalian distances (Baker and Bradley (2006). Additionally, cytogenetic studies have revealed karyotypic differences among these lineages (Silva et al., 2015; Oliveira da Silva et al., 2017, 2019). These, along with qualitative-morphological data reported in our study, provide evidence of reproductive isolation and nuclear-gene divergence, respectively.

Carotid circulation patterns have long been considered a reliable character for diagnosing sigmodontine species (Voss, 1988; Carleton and Musser, 1989; Voss and Carleton, 1993; Steppan, 1995; Carleton and Olson, 1999; Weksler, 2006; Hurtado and Pacheco, 2017; and Sánchez-Vendizú et al., 2018). However, intraspecific polymorphism in this character was reported by Voss (1991), and our observations provide additional evidence that oryzomyine species can be polymorphic for carotid circulatory traits. Carotid polymorphisms in *N. marajoara* and *N. xingu* may be related to the recency of speciation events from which these lineages arose, as evidenced by their minimal genetic divergence. Because these are not the only congeneric species that exhibit carotid polymorphisms (T.B.F.S., unpublished), observations of sample differences in carotid traits should be interpreted cautiously unless accompanied by other evidence of taxonomic divergence.

The discovery of new species of *Neacomys* in southeastern Amazonia is not unexpected, in view of similar recent discoveries in western and northeastern Amazonia (Patton et al., 2000; Voss et al., 2001; Hurtado and Pacheco, 2017; and Sanchez-Vendizú et al., 2018) and previous reports of karyotypic variation and genetic divergence among southeastern forms (Patton et al., 2000; Catzeflis and Tilak, 2009; Silva et al., 2015; Oliveira da Silva et al., 2017; Hurtado and Pacheco, 2017; and Sanchez-Vendizú et al., 2018). Although southeastern Amazonia has long been accessible to collectors, our study underscores the fact that faunal inventories and taxonomic studies are still needed in this region, which is among the most extensively deforested and environmentally threatened parts of the Amazonian biome, due to industrial agriculture, road construction, mining, and hydroelectric dams (Fearnside, 1989, 2005; Gascon et al., 2001).

ACKNOWLEDGMENTS

We are grateful to the following curators and collection managers for permitting access to specimens under their care: Robert Voss and Eileen Westwig (at AMNH), Kris Helgen and Darrin Lunde (USNM), Burton Lim (ROM), Priscilla Tucker and Cody Thompson (UMMZ), Roberto Portella (BMNH), John R. Wible and Susan B. McLaren (CM), Manuel Ruedi (MHNG), Fernando Pacheco (UNB), Suely Marques-Aguiar (MPEG), Manoel Santos Filho (UNEMAT), Cláudia Costa (PUC-MG). This study was supported by the Fundação de Amparo à Pesquisa do Estado de Mato Grosso (FAPEMAT/PRONEM #477017/2011 to R.V.R). I.P.F. was supported by the Project CNPq/SISBIOTA-BioPHAM 563348/2010. T.B.F.S. was partially supported by the Coordenação de Aperfeiçoamento de Pessoal de Nível Superior–Brasil (CAPES), Finance Code 001; by an Ernst Mayr Grant from the Museum of Comparative Zoology at Harvard University, Cambridge, MA; by small grants from the American Museum of Natural History (New York) and the Muséum d'Histoire Naturelle (Geneva); by the Programa de Pós-Graduação em Zoologia da Universidade Federal de Mato Grosso (PPGZOO/UFMT); and by scholarships from the Conselho Nacional de Desenvolvimento Científico e Tecnológico (CNPq) and the Ministério da Ciência, Tecnologia, Inovações e Comunicações (MCTIC) (300617/2020-8).

T.B.F.S. is additionally grateful to Marinez I. Marques (head of the PPGZOO, 2014-2016) who provided financial support to this study, and to Karl-L. Schuchmann. We thank Luan Silva for helping with the layout of figure 5; Silvia Pavan for kindly providing sequence data from MPEG 45483; Cleuton L. Miranda for reading a previous version of the manuscript; and Guilherme Garbino, Robert Voss, and Pablo Teta who made several helpful suggestions for its improvement. T.B.F.S. wants to express his gratitude and love for his father, Antonio F. Semedo Fernandes, who passed away during the completion of this study.

REFERENCES

Aljanabi, S.M., and I. Martinez. 1997. Universal and rapid salt-extraction of high-quality genomic DNA for PCR-based techniques. Nucleic Acids Research 25: 4692–4693.

Altekar, G., S. Dwarkadas, J.P. Huelsenbeck, and F. Ronquist. 2004. Parallel Metropolis-coupled Markov chain Monte Carlo for Bayesian phylogenetic inference. Bioinformatics 20: 407–415.

Baker, R.J., and R.D. Bradley. 2006. Speciation in mammals and the genetic species concept. Journal of Mammalogy 87: 643–662.

Brandão, M.B. et al. 2019. Mammals of Mato Grosso, Brazil: Annotated species list and historical review. Mastozoología Neotropical, 26: 263–307.

Cabrera, A. 1961. Catálogo de los mamíferos de América del Sur. Revista del Museo Argentino de Ciencias Naturales "Bernardino Rivadavia," Ciencias Zoológicas 42: xxii + 309–732.

Carleton, M.D., and G.G. Musser. 1989. Systematic studies of oryzomine rodents (Muridae, Sigmodontinae): a synopsis of *Microryzomy*s. Bulletin of the American Museum of Natural History 191: 1–83.

Carleton, M.D., and S.L. Olson. 1999. Amerigo Vespucci and the rat of Fernando de Noronha: a new genus and species of Rodentia (Muridae: Sigmodontinae) from a volcanic island off Brazil's continental shelf. American Museum Novitates 3256: 1–59.

Catzeflis, F., and M. Tilak. 2009. Molecular systematic of Neotropical spiny mice (*Neacomys*: Sigmodontinae, Rodentia) from the Guianan Region. Mammalia 73: 239–247.

Di-Nizo, C.B., K.R.S. Banci, Y. Sato-Kuwabara, and M.J.J. Silva. 2017. Advances in cytogenetics of Brazilian rodents: cytotaxonomy, chromosome evolution and new karyotypic data. Comparative Cytogenetics 11:833–89.

Fearnside, P.M. 1989. The charcoal of Carajas: Pig-iron smelting threatens the forests of Brazil's Eastern Amazon Region. Ambio, 18: 141–143.

Fearnside, P.M. 2005. Deforestation in Brazilian Amazonia: History, rates and consequences. Conservation Biology, 19: 680–688.

Flores, T., R.V. Rossi, and I. Sampaio. 2010. Morphological and molecular diversity in the species of *Oecomys* Thomas, 1906 (Rodentia: Cricetidae) from eastern Amazon in Brazil. Master's thesis, Museu Paraense Emilio Goeldi, Belém, Pará.

Gardner, A.L. (editor). 2008 ("2007"). Mammals of South America, Vol. I: Marsupials, xenarthrans, shrews, and bats. Chicago: University of Chicago Press.

Gascon, C., Bierregaard, Jr., Laurance R.O. and J, rankin-de-merona. 2001. Deforestation and forest fragmentation in the Amazon. *In* R.O. Bierregaard Jr, C. Gascon, T.E. Lovejoy, and R. Mesquita (editors), Lessons from Amazonia: 22–30. The ecology and conservation of a fragmented forest. New Haven, CT: Yale University Press.

Guindon, S., et al. 2010. New algorithms and methods to estimate maximum-likelihood phylogenies: assessing the performance of PhyML 3.0. Systematic Biology 59: 307–321.

Hershkovitz, P. 1940. Four new oryzomyine rodents from Ecuador. Journal of Mammalogy 21: 78–84.

Huelsenbeck, J.P., and F. Ronquist. 2001. MRBAYES: Bayesian inference of phylogenetic trees. Bioinformatics 17: 754–755.

Hurtado, N., and V. Pacheco. 2017. Revision of *Neacomys spinosus* (Thomas, 1882) (Rodentia: Cricetidae) with emphasis on Peruvian populations and the description of a new species. Zootaxa 4242: 401–440.

Lanfear, R., P.B. Frandsen, A.M. Wright., T. Senfeld, and B. Calcott. 2017. PartitionFinder 2: new methods for selecting partitioned models of evolution for molecular and morphological phylogenetic analyses. Molecular Biology and Evolution 34: 772–773.

Miller, M.A., W. Pfeiffer, and T. Schwartz. 2010. Creating the CIPRES science gateway for inference of large phylogenetic trees. Proceedings of the 2010 Gateway Computing Environments Workshop (GCE). [doi: 10.1109/GCE.2010.5676129]

Musser, G.G., and M.D. Carleton. 2005. Superfamily Muroidea. *In* D.E. Wilson, and D.M. Reeder (editors), Mammals species of the world, a taxonomic and geographic reference: 894–1531. Baltimore: Johns Hopkins University Press.

Oliveira da Silva, W., et al. 2017. Chromosomal diversity and molecular divergence among three undescribed species of *Neacomys* (Rodentia, Sigmodontinae) separated by Amazonian rivers. PLoS ONE 12: 1–19.

Oliveira da Silva, W., et al. 2019. Chromosomal phylogeny and comparative chromosome painting among *Neacomys* species (Rodentia, Sigmodontinae) from eastern Amazonia. Bmc Evolutionary Biology 19: 1–13.

Patton, J.L., M.N.F. da Silva, and J.R. Malcolm. 2000. Mammals of the rio Juruá and the evolutionary and ecological diversification of Amazonia. Bulletin of the American Museum of Natural History 244: 1–306.

Patton, J.L., U.F.J. Pardiñas, and G. D'Elía. 2015. Mammals of South America, vol. 2: Rodents. Chicago: University of Chicago Press.

Paynter, R.A., Jr. 1993. Ornithological gazetteer of Ecuador. Cambridge, MA: Museum of Comparative Zoology (Harvard University).

Paynter, R.A., Jr., and M.L. Traylor, Jr. 1991. Ornithological gazetteer of Brazil [2 vols.]. Cambridge, MA: Museum of Comparative Zoology (Harvard University).

Percequillo, A.R., M. Weksler, and L.P. Costa. 2011. A new genus and species of rodent from the Brazilian Atlantic Forest (Rodentia: Cricetidae: Sigmodontinae: Oryzomyini), with comments on oryzomyine biogeography. Zoological Journal of the Linnean Society 161: 357–390.

Prado, J.R., and A.R. Percequillo. 2013. On the geographic distribution of the genera of tribe Oryzomyini on South America, with some comments on the patterns of diversity and Reig's areas of original differentiation. Arquivos de Zoologia 44: 1–124.

Ronquist, F., and J.P. Huelsenbeck. 2003. MRBAYES 3: Bayesian phylogenetic inference under mixed models. Bioinformatics 19: 1572–1574.

Ronquist, F., et al. 2012. MrBayes 3.2: efficient Bayesian phylogenetic inference and model choice across a large model space. Systematic Biology 61: 539–542.

Sánchez-Vendizú, P., V. Pacheco and D. Vivas-Ruiz. 2018. An introduction to the systematics of small-bodied *Neacomys* (Rodentia: Cricetidae) from Peru with descriptions of two new species. American Museum Novitates 3913: 1–38.

Silva, J.M.C., A.B. Rylands and G.A.B. Fonseca 2005. O destino das áreas de endemismo da Amazônia. Megadiversidade 1: 124–131.

Silva, W.O., et al. 2015. Diversity and karyotypic evolution in the genus *Neacomys* (Rodentia, Sigmodontinae). Cytogenetic and Genome Research 146: 1–10.

Smith, M.F., and J.L. Patton. 1993. The diversification of South American murid rodents: evidence from mitochondrial DNA sequence data for akodontine tribe. Biological Journal of Linnean Society 50: 149–177.

Steppan, S.J. 1995. Revision of the tribe Phyllotini (Rodentia: Sigmodontinae), with a phylogenetic hypothesis for the Sigmodontinae. Fieldiana Zoology (New Series) 80: 1–112.

Tamura, K., et al. 2011. MEGA6: molecular evolutionary genetics analysis using maximum likelihood, evolutionary distance, and maximum parsimony methods. Molecular Biology and Evolution 28: 2731–2739.

Thompson, J.D., D.G. Higginsand, and T.J. Gibson. 1994. CLUSTAL W: improving the sensitivity of progressive multiple sequence alignment through sequence weighting, position-specific gap penalties and weight matrix choice. Nucleic Acids Research 22: 4673–4680.

Voss, R.S. 1988. Systematics and ecology of ichthyomyine rodents (Muroidea): patterns of morphological evolution in a small adaptive radiation. Bulletin of the American Museum of Natural History 188 (2): 259–493.

Voss, R.S. 1991. An introduction to the Neotropical muroid rodent genus *Zygodontomys*. Bulletin of the American Museum of Natural History 210: 1–113.

Voss, R.S., and M.D. Carleton. 1993. A new genus for *Hesperomys molitor* Winge and *Holochilus magnus* Hershkovitz (Mammalia, Muridae) with an analysis of its phylogenetic relationships. American Museum Novitates 3085: 1–39.

Voss, R.S., D.P. Lunde, and N.B. Simmons. 2001. The mammals of Paracou, French Guiana: a Neotropical lowland rainforest fauna. Part 2. Nonvolant species. Bulletin of the American Museum of Natural History 263: 1–236.

Weksler, M. 2003. Phylogeny of Neotropical oryzomyine rodents (Muridae: Sigmodontinae) based on the nuclear IRBP exon. Molecular Phylogenetics and Evolution 29: 331–349.

Weksler, M. 2006. Phylogenetic relationships of oryzomyine rodents (Muridae: Sigmodontinae): separate and combined analyses of morphological and molecular data. Bulletin of the American Museum of Natural History 296: 1–149.

Weksler, M., and C. Bonvicino. 2015. Genus *Neacomys* Thomas, 1900. *In* J.L. Patton, U.F.J. Pardiñas, and G. D'Elía (editors), Mammals of South America. Chicago: University of Chicago Press.

Woodman, N., et al. 1991. Annotated checklist of the mammals of Cuzco Amazonico, Peru. Occasional Papers of the Museum of Natural History University of Kansas 145:1–12.

Zwickl, D.J. 2006. Genetic algorithm approaches for the phylogenetic analysis of large biological sequence datasets under the maximum likelihood criterion. Ph.D. dissertation, University of Texas at Austin, Austin.

APPENDIX 1

Specimens Examined

The localities of specimens from the Dubosti Group that we examined and from which we analyzed sequence data are listed below. The largest administrative units within each country (state, department, or province) are italicized. Verbatim locality names are placed in quotes, but others have been emended for brevity and to conform with current geographic usage. For each locality we provide geographic coordinates and the collection number of the voucher specimens examined. Numbers identify locality symbols plotted on map (fig. 5). The paratypes of our new species are designated here.

BRAZIL

1. *Amapá*, Serra do Navio km 190 efa. (00˚59'S, 52˚03'W; USNM 461589; *N. dubosti*).
2. *Amapá*, Rio Amapari (00˚59'S, 52˚03'W; USNM 461573, 461587; *N. dubosti*).
3. *Pará*, Almeirim Municipality, Reserva Biológica Maicuru (00˚50'N, 53˚56'W; CN 240; *N. dubosti*).
4. *Pará*, Chaves municipality, Marajó Island, Tauari Farm (00˚39'S, 50˚11'W; MPEG 40429, 40431, 40434, 40435, 40439–40441, 40443, 40446 [paratypes]; MPEG 40432 [holotype]; *N. marajoara*).
5. *Pará*, Mangabal community on right bank of Rio Tapajós, Itaituba (5˚35'S, 57˚7'W; UFPA 1736 [paratype]; *N. vossi*).
6. *Pará*, Itaituba Municipality, Boca do Rato on right bank of Rio Tapajós (6˚7'S, 57˚36'W; UFPA 1391, 1520, 1577 [paratypes]; UFPA 1583 [holotype]; *N. vossi*).
7. *Pará*, Itaituba, Mamãe-anã (Canta-galo) on right bank of Rio Tapajós (5˚48'S, 57˚24'W; UFPA 1277, 1284, 1487, 1647, 1654 [paratypes]; *N. vossi*).
8. *Pará*, Itaituba (5˚40'S, 57˚00'W; UFPA 1467, JB 27; *N. vossi*).
9. *Pará*, Itaituba, São Martins on right bank of Rio Tapajós (6˚07'S, 57˚36'W; UFPA 1691 [paratype]; *N. vossi*).
10. *Pará*, Itaituba, Jacaré on right bank of Rio Tapajós (5˚41'S, 57˚14'W; UFPA 1444 [paratype]; *N. vossi*).
11. *Pará*, 18 km south and 19 km west of Altamira- Agrovila da União (03˚22'S, 52˚23'W; USNM 521468, 521539; *N. vossi*).
12. *Pará*, Itaituba, Br 230, Itaituba-Jacareacanga Km 212 on Transamazonica Highway (5˚40'S, 56˚45'W; USNM 545957–545959, 545960–545964; *N. vossi*).
13. *Pará*, Marabá Municipality, Flona Tapirapé-Aquiri (5˚51'S, 50˚31'W; UFMT 1273, 1275 [paratypes]; MPEG 39901, 41804, 41805, 41991, 41996, 42019; MPEG-PSA 46, 69 [paratypes]; UFMT 1268: [holotype]; *N. xingu*).
14. *Pará*, East bank Rio Xingu 52 km SSW Altamira (3˚39'S, 52˚22'W; USNM 549553; *N. xingu*).
15. *Pará*, 54 km south and 150 km west of Altamira (3˚41'S, 51˚45'W; USNM 519180, 521464–521467; *N. xingu*).

16. *Pará*, Flona Carajás, Parauapebas (6˚3'S, 50˚35'W; MCN-M 1401–1404, 1443 [paratypes]; *N. xingu*).
17. *Pará*, left bank of Rio Tapajós (5˚17'S, 57˚8'W; MPEG 42838, 42901; *Neacomys* sp. 2).
18. *Pará*, Juruti (2˚09'S, 56˚5'W; JUR 19, 42, 82; *Neacomys* sp. 2).
19. *Pará*, Penedo on left bank of Rio Tapajós (5˚30'S, 57˚6'W; UFPA 1227, 1413, 1417, 1530; *Neacomys* sp. 2).
20. *Pará*, Reserva Biológica Maicuru. 00˚50'N. 53˚56'W (CN 240: *Neacomys dubosti*).

FRENCH GUIANA

21. Paracou near Sinnamary (05˚17'N. 52˚55'W; AMNH 267569 [holotype]; *N. dubosti*)
22. Cacao, Roura, Cayenne (04˚34'N, 52˚27'W; MHNG 1963.025: *N. dubosti*).
23. Route de Kaw, Cayenne (04˚36'N, 52˚15'W; MHNG 1894.013: *N. dubosti*).

SURINAM

24. *Nickerie District*, Sipaliwini Airstrip (02˚02'N, 56˚07'W; CM 76846: *N. dubosti*).
25. *Sipaliwini*, Werehpai Camp (02˚23'N, 56˚42'W: ROM 120726: *N. dubosti*).
26. *Sipaliwini*, Iconja Landing on Sipaliwini River (01˚59'N, 56˚05'W: ROM 120288: *N. dubosti*).
27. *Marowijne*, Oelemarie (03˚06'N, 54˚31'W; CM 76835–76837, 76839, 76840, 76842–76844; *N. dubosti*).

APPENDIX 2

Phylogenetic Relationships of *Neacomys* Based on Maximum-Likelihood Analysis

(For simplicity, clades shared with our Bayesian results [in fig. 2A–C] are cartooned. Branch support values are bootstrap frequencies.)

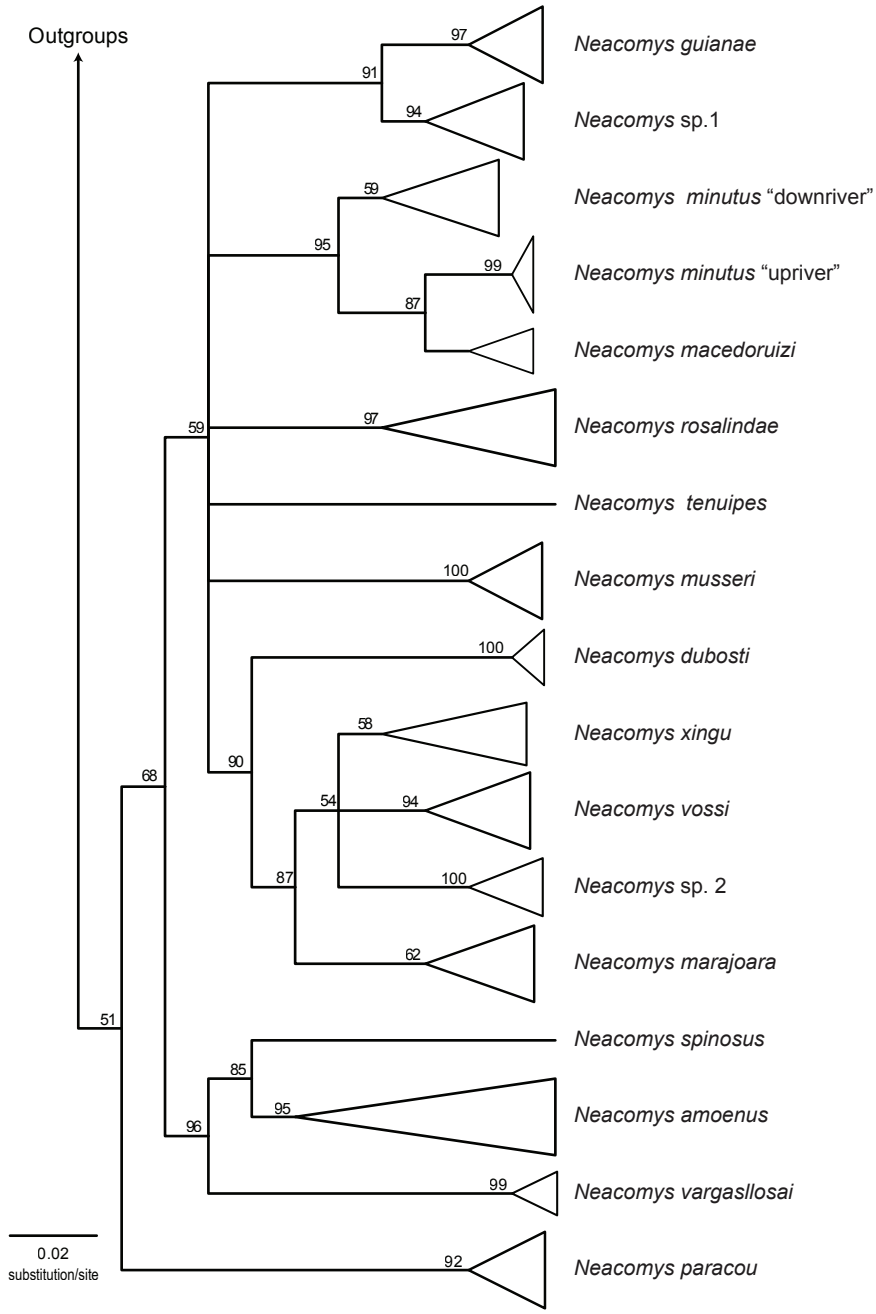

APPENDIX 3

Results of Principal Components Analyses of Species in the Dubosti Group of *Neacomys*

	dubosti vs marajoara		*dubosti vs vossi*		*dubosti vs xingu*		*marajoara vs vossi*		*marajoara vs xingu*		*vossi vs xingu*	
	PC1	PC2	PC1	PC2	PC1	PC2	PC1	PC2	PC1	PC2	PC1	PC2
BH	0.54	0.47	0.80	0.23	0.59	0.57	0.30	-0.79	0.04	-0.65	0.38	0.27
BIF	0.65	-0.09	0.41	0.15	0.68	-0.03	0.09	0.63	0.52	0.40	0.21	-0.02
BM1	0.73	0.37	0.62	0.30	0.83	0.14	0.38	0.33	0.70	-0.24	0.49	0.50
BPR	0.52	0.36	0.70	-0.03	0.85	-0.07	0.76	0.22	0.66	0.05	0.57	0.30
BZP	0.71	0.26	0.64	0.31	0.71	0.23	-0.09	0.25	0.77	-0.14	0.66	0.34
BB	0.29	-0.49	0.70	-0.37	0.55	-0.21	0.20	0.14	0.28	-0.14	0.44	-0.28
CIL	0.87	-0.37	0.93	-0.19	0.92	-0.19	0.88	-0.12	0.90	0.11	0.90	-0.18
LCIB	0.25	0.35	0.13	0.60	0.19	0.63	0.32	-0.67	0.69	-0.17	0.73	-0.23
LIB	0.47	0.13	0.53	0.44	0.64	0.20	0.06	0.26	0.42	0.53	0.32	-0.17
LD	0.69	-0.40	0.88	-0.26	0.87	-0.33	0.75	0.22	0.58	0.60	0.68	-0.49
LIF	0.23	-0.68	0.48	-0.69	0.22	-0.56	0.82	-0.20	0.15	0.57	0.45	-0.65
LLD	0.50	0.25	0.40	0.38	0.43	0.07	0.05	0.33	0.26	0.18	0.22	0.17
LLM	0.40	0.26	0.71	0.16	0.68	0.39	0.49	-0.04	0.66	-0.53	0.70	0.23
LM	0.48	0.54	0.78	0.28	0.73	0.47	0.28	-0.54	0.68	-0.43	0.76	0.40
LN	0.53	-0.48	0.77	-0.46	0.67	-0.57	0.81	0.28	0.86	0.05	0.89	-0.14
LPB	0.48	0.24	0.51	0.26	0.67	0.05	0.23	0.10	0.69	-0.21	0.49	0.49
MB	0.79	0.02	0.86	0.20	0.83	0.27	0.21	-0.71	0.71	-0.31	0.75	0.07
OL	0.75	-0.43	0.80	-0.25	0.72	-0.42	0.51	0.12	0.68	0.34	0.75	-0.39
RB	0.45	0.20	0.36	0.07	0.34	-0.28	0.68	0.40	0.59	-0.08	0.58	0.39
RL	0.66	-0.33	0.74	-0.38	0.70	-0.44	0.78	0.23	0.83	0.30	0.79	-0.17
ZB	0.85	0.00	0.92	0.07	0.87	0.12	0.79	-0.28	0.81	-0.05	0.88	-0.07
% Variance	46.98	12.62	47.22	11.31	35.58	13.33	28.97	15.48	41.20	12.35	41.13	10.94

All issues of *Novitates* and *Bulletin* are available on the web (http://digitallibrary.amnh.org/dspace). Order printed copies on the web from:
http://shop.amnh.org/a701/shop-by-category/books/scientific-publications.html

or via standard mail from:

American Museum of Natural History—Scientific Publications
Central Park West at 79th Street
New York, NY 10024

♾ This paper meets the requirements of ANSI/NISO Z39.48-1992 (permanence of paper).